



Pre- and early postnatal enriched environmental experiences prevent neonatal hypoxia-ischemia late neurodegeneration via metabolic and neuroplastic mechanisms

Luz Elena Durán-Carabali¹  | Felipe Kawa Odorcyk¹ | Samuel Greggio² |
 Gianina Teribele Venturin² | Eduardo Farias Sanches³ | Guilherme Garcia Schu³ |
 Andrey Soares Carvalho⁴ | Thales Avila Pedroso⁵ | Natividade de Sá Couto-Pereira⁴  |
 Jaderson Costa Da Costa² | Carla Dalmaz^{3,4,5} | Eduardo Rigon Zimmer^{6,7} |
 Carlos Alexandre Netto^{1,3,5}

¹Graduate Program in Biological Sciences: Physiology, Instituto de Ciências Básicas da Saúde (ICBS), Universidade Federal do Rio Grande do Sul, Porto Alegre, Brazil

²Preclinical Research Center, Brain Institute (Brains) of Rio Grande do Sul, Porto Alegre, Brazil

³Graduate Program in Biological Sciences: Biochemistry, Instituto de Ciências Básicas da Saúde, Universidade Federal do Rio Grande do Sul, Porto Alegre, Brazil

⁴Graduate Program in Biological Sciences: Neuroscience, Instituto de Ciências Básicas da Saúde, Universidade Federal do Rio Grande do Sul, Porto Alegre, Brazil

⁵Department of Biochemistry, Universidade Federal do Rio Grande do Sul, Porto Alegre, Brazil

⁶Graduate Program in Biological Sciences: Pharmacology and Therapeutics, Instituto de Ciências Básicas da Saúde, Universidade Federal do Rio Grande do Sul, Porto Alegre, Brazil

⁷Department of Pharmacology, Universidade Federal do Rio Grande do Sul, Porto Alegre, Brazil

Correspondence

Luz Elena Durán-Carabali, Graduate Program in Biological Sciences: Physiology, Instituto de Ciências Básicas da Saúde (ICBS), Universidade Federal do Rio Grande do Sul, Porto Alegre, Brazil.
 Email: Luzeled67@gmail.com

Carlos Alexandre Netto, Department of Biochemistry, Universidade Federal do Rio

Abstract

Prenatal and early postnatal periods are important for brain development and neural function. Neonatal insults such as hypoxia-ischemia (HI) causes prolonged neural and metabolic dysregulation, affecting central nervous system maturation. There is evidence that brain hypometabolism could increase the risk of adult-onset neurodegenerative diseases. However, the impact of non-pharmacologic strategies to attenuate HI-induced brain glucose dysfunction is still underexplored. This study investigated the long-term effects of early environmental enrichment in metabolic, cell, and functional responses after neonatal HI. Thereby, male Wistar rats were divided according to surgical procedure, sham, and HI (performed at postnatal day 3), and the allocation to standard (SC) or enriched condition (EC) during gestation and lactation periods. In-vivo cerebral metabolism was assessed by means of [¹⁸F]-FDG micro-positron emission tomography, and cognitive, biochemical, and histological analyses were performed in adulthood. Our findings reveal that HI causes a reduction in glucose metabolism and glucose transporter levels as well as hyposynchronicity in metabolic brain networks. However, EC during prenatal or early postnatal period attenuated these metabolic disturbances. A positive correlation was observed between [¹⁸F]-FDG values and volume ratios in adulthood, indicating that preserved tissue by EC is metabolically active. EC promotes better cognitive scores, as well as down-regulation of amyloid precursor protein in the parietal cortex and hippocampus of HI animals. Furthermore, growth-associated protein 43 was up-regulated in the cortex of EC animals. Altogether, results presented support that EC during gestation and lactation period can reduce HI-induced impairments that may contribute to functional decline and progressive late neurodegeneration.

Abbreviations: APP, amyloid precursor protein; BBB, blood-brain barrier; CNS, central nervous system; EC, enriched condition; GAP-43, growth-associated protein 43; GAPDH, glyceraldehyde-3-phosphate dehydrogenase; GLUT, glucose transporter; HI, hypoxia-ischemia; MBN, metabolic brain network; MCT, monocarboxylic acid transporter; MicroPet, micro-positron emission tomography; PND, postnatal day; SC, standard condition; SUVr, Relative standardized uptake value.

Grande do Sul (UFRGS), Rua Ramiro Barcelos 2600, anexo. CEP 90035-003, Porto Alegre, RS, Brazil.

Emails: netto@gabinete.ufrgs.br

Funding information

Conselho Nacional de Desenvolvimento Científico e Tecnológico, Grant/Award Number: 01/2016 and 405470/2016-9; Coordenação de Aperfeiçoamento de Pessoal de Nível Superior (CAPES)

KEYWORDS

[18F]-FDG microPET, APP, brain development, brain metabolism, cognitive impairment, Environmental enrichment, GAP-43

1 | INTRODUCTION

Prolonged dysregulation in energy metabolism during the perinatal period, increases brain vulnerability and compromises its maturation, and is responsible for varying degrees of functional deficits (McKenna et al., 2015; Nehlig, 2004). Brain metabolism undergoes modifications in several aspects at the early postnatal period, such as glucose consumption, glucose transporter (GLUT), and monocarboxylate transporter (MCT) levels (Brekke et al., 2014, 2017). Previous studies indicate that glucose brain hypometabolism after neonatal HI may predict the degree of damage and, consequently, the dimension of behavioral impairments (Marik et al., 2009). Early metabolic changes may affect the utilization of this energy substrate since glucose is the primary energy source for the adult brain.

Growing evidence suggests that neonatal brain insults can increase the risk of adult-onset neurodegenerative diseases (Faa et al., 2014; Martin et al., 2019; Nalivaeva et al., 2018). Data regarding Alzheimer's disease indicate that brain glucose hypometabolism occurs before the onset of cognitive impairment and contributes to the progression of neuropathological events (Cunnane et al., 2012). Moreover, neonatal brain damage and neurodegenerative disease share common mechanisms of injury, such as blood-brain barrier (BBB) failure, mitochondrial dysfunction, excitotoxicity, inflammation, and cell death. Neuroimaging techniques, as micro-positron emission tomography (microPET), allow for measurements of local glucose metabolism using the ^{18}F -fluorodeoxyglucose (^{18}F -FDG). This technique has been widely used to investigate brain metabolism in several central nervous system (CNS) disorders as an index of synaptic function, and it is currently acknowledged as a biomarker of neurodegeneration (Jack et al. 2018; Zimmer et al., 2017; Stoessl, 2017).

Neonatal HI has a significant impact in the levels of protein related to the development and function of the CNS. The amyloid precursor protein (APP) and growth-associated protein 43 (GAP-43) are functionally important for synapses reorganization as ensue in learning processes and memory consolidation (Benowitz & Routtenberg, 1997; Hefter et al., 2019), and are amongst the proteins affected by HI. It was reported that brain glucose hypometabolism may induce changes in the levels of APP and affect its role in axonal transport and turnover, thus increasing the risk of early-onset neurodegenerative conditions such as Alzheimer's disease (Costantini et al., 2008; Stokin & Goldstein, 2006). Similarly, GAP-43 levels decline has been observed in conditions related to cerebral glucose

metabolism dysfunction and as consequences of the axonal degeneration (Bogdanovic et al., 2000; Coleman et al., 1992). Furthermore, abnormal synaptic and neuritic changes in aged animals are accompanied by the accumulation of APP and aberrant levels of GAP-43 (Masliah et al., 1992; Masliah & Terry, 1993). Thereby, alterations in these protein levels as a consequence of the HI insult might contribute to the cognitive dysfunction and the neurodegeneration cascade (Chen et al., 2012; Nalivaeva et al., 2018; Wu et al., 2016).

The above-mentioned evidence raises several questions about the relevance of early interventions to prevent late neurodegeneration processes leading to cognitive deficits, aberrant plasticity, and glucose hypometabolism, that may be triggered by the HI insult. Environmental enrichment is an approach able to modify neural development and functional performance (Bayne, 2018; Kempermann, 2019; McDonald et al., 2018). Recent studies also suggest that environmental enrichment during brain development favors processes of endogenous protection to the CNS [for review (Sale, 2018)] and is a promising strategy for the prevention of cell damage after brain insults [for review (Hassell et al., 2015; Netto et al., 2018)]. Previous reports show that gestational and early postnatal enriched housing protocols attenuate morphological damage and behavioral impairments caused by the neonatal HI (Durán-Carabali et al., 2017, 2019; Rojas et al., 2013; Zhang et al., 2016). Nevertheless, the long-term potential contributions of early environmental interventions to modulate brain glucose metabolism are not yet demonstrated. This investigation could provide important insights on HI pathophysiology and improve the development of potential therapeutic approaches for neonatal HI. Therefore, this study aims to evaluate the long-term effects of early environment enrichment, during gestation and lactation, in neonates undergoing HI and assessed for brain metabolism and cognition in adulthood. We hypothesized that maternal enrichment induces metabolic effects in the pregnant rat that will be passed on to the offspring, and that prolonged stimulation during the lactation period are capable of impacting brain energy metabolism and, consequently, synaptic proteins and cognitive performance.

2 | METHODS

2.1 | Animals and rearing environment

Experimental procedures were performed in accordance with the guidelines of the Brazilian Society of Science in Laboratory

Animals and the recommendations of the Council for International Organizations of Medical Sciences. This study was not pre-registered; however, protocols were approved by the animal care committee from the Universidade Federal do Rio Grande do Sul-UFRGS (#37304). Male rats used in this study were offspring of Wistar female rats supplied by the colony of the Biochemistry Department, UFRGS (<http://www.ufrgs.br/creal/>) and kept in the animal house of the same Department. No randomization was performed to allocate female rats in the study. Therefore, 20 female Wistar rats were assigned to either standard (SC, $n = 10$) or enriched housing condition (EC, $n = 10$) and mated during proestrus/estrus cycles. The day on which sperm-positive vaginal smear was observed was denominated pregnancy day 1. Animals of the SC group were raised in $18 \times 42 \times 34$ cm cages, in groups of four females during pregnancy and one litter per cage before weaning. The EC contained eight pregnant rats, or two litters during lactation, in a large rectangular cage ($120 \times 80 \times 100$ cm), with different stimuli inside, like running wheels, ramps, and a variety of toys. The stimuli were changed twice a week. For animals in both conditions, water and food were provided ad libitum. Rats were exposed to a temperature-controlled, 12-hr light/dark-cycle facility and the bedding was changed weekly. After birth, litters were allocated in one of four housing conditions (Durán-Carabali et al., 2019) as shown in Figure 1:

- Standard condition during gestation and lactation period (SC-SC). This is the environmental control group;
- Standard condition during gestation followed by enriched condition during lactation period (SC-EC);
- Enriched condition during gestation followed by standard condition during lactation period (EC-SC);
- Enriched condition from gestation to weaning (EC-EC).

This experimental design was used to evaluate critical periods of the EC and to determine whether the combination of maternal

and neonatal experiences is necessary, or if pre- and early postnatal exposures alone are enough, to confer brain protection.

On the third postnatal day (PND3) male pups were submitted to neonatal HI procedure. For the HI procedure, it was decided that the first operated pup would be assigned to the HI group and the second to the control group, third to the HI group and so on. In order to easily identify the animals 10ul of non-toxic ink (Acrilex) was injected into the animal's paw with an insulin needle (6 mm), while the animals were anesthetized. Different ink colors were used to identified distinct environmental conditions. Rats were weaned on PND 23 and remained in SC for twelve weeks. Brain tissue was collected on day 72. A cohort of seven to ten male rats per group was used for in vivo [^{18}F]-FDG microPET imaging to access brain glucose metabolism and histological analysis (evaluated on PND 60 and 72, respectively). A second cohort was used for biochemical analysis (six to eight animals per housing condition and surgical procedure). Hippocampus-dependent memory was evaluated in both cohorts from PND 65 to 70. All the experiments were conducted during the light cycle (between 8 a.m. and 1 p.m.).

Metabolic, biochemical, and behavioral assessments were performed in male rats because of their higher brain vulnerability to the HI insult, greater long-term cognitive deficits, and smaller response to therapeutic interventions (Hill & Fitch, 2012). Female pups were excluded from this study and returned to the animal colony to an adequate destination. In addition, the health of animals during the whole experiment was considered as an inclusion/exclusion criterion: only healthy rats were used for further analysis. Animals were examined daily by technical staff to look for evidence of poor health. Six male pups died during the HI procedure (mortality rate of 5%), regardless of environmental rearing conditions (HI_SC-SC: 2 animals, HI_SC-EC: 1 animal, HI_C-SC: 2 animals, and HI_EC-EC: 1 animal). The animals that died during the experiment were not replaced. Rats used for MicroPET scanning also went on to behavioral testing and post-mortem histological analysis, in an attempt to reduce the number of used animals. Moreover, efforts were made to

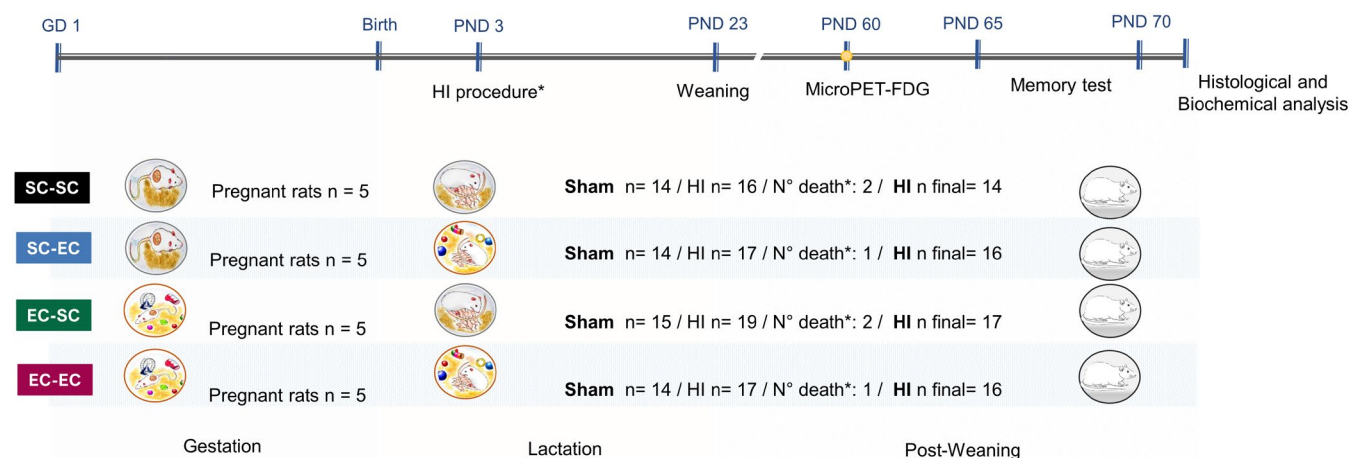


FIGURE 1 Experimental timeline protocol from prenatal period to adulthood in Wistar rats. GD: gestational day; HI: hypoxia-ischemia; PND: postnatal day; SC-SC: standard condition during gestation and lactation period; SC-EC: standard condition during gestation followed by enriched condition during lactation period; EC-SC: enriched condition during gestation followed by standard condition during lactation; EC-EC: enriched condition from gestation to weaning. *Time point of animal death



minimize animal's suffering such as the use of an inhaled anesthetic agent (isoflurane) during HI procedure and imaging scans, based on the benefits of rapid induction and recovery. Animals were tested by an experimenter unaware of group allocation on the microPET scans and Morris water maze (MWM) test. Likewise, image reconstruction, biochemical, and morphological analysis were performed by a blinded experimenter.

2.2 | Surgical procedure

The Rice-Vannucci model for the induction of neonatal HI was performed in male rats at PND 3 (Stadlin et al., 2003). Pups were anesthetized with 4% inhalatorial isoflurane and maintained with 2% of the anesthetic during surgical procedures. After performing a vertical midline incision on the neck, the right common carotid artery was isolated from adjacent structures and double ligated with a 4.0 silk. In the sham group (surgical control), a similar incision was made in the neck, but the artery was not ligated. A heat pad was used to maintain the animal's body temperature at 36°C during surgery. Neonates remained with their dams for 2hr for surgical recovery. After that, the pups were placed in the hypoxia chamber, with 8% oxygen and balanced nitrogen (92%) for 180 min, under controlled temperature. Animals of the sham groups were kept in a similar chamber and exposed to room air. At the end of hypoxia, all rats were returned to dams in their respective housing condition (Durán-Carabali et al., 2019). Thereby, rats of each housing condition were assigned to sham or HI group, comprising eight experimental groups: (a) Sham_SC-SC ($n = 14$); (b) HI_SC-SC ($n = 14$); (c) Sham_SC-EC ($n = 14$); (d) HI_SC-EC ($n = 16$); (e) Sham_EC-SC ($n = 15$); (f) HI_EC-SC ($n = 17$); (g) Sham_EC-EC ($n = 14$) and (h) HI_EC-EC ($n = 16$).

2.3 | Micro-positron emission tomography imaging and analysis

[¹⁸F]-FDG microPET scanning was conducted to evaluate the long-term effects of housing condition in the glucose brain metabolism of animals suffering neonatal HI and their respective control. The Triumph™ micro-PET equipment (LabPET-4, TriFoil Imaging) was used. PET image acquisition and preprocessing protocols were performed as described previously (Bellaver et al., 2019). Briefly, on the PND 60, male rats were anesthetized with 4% of isoflurane mixed with medical oxygen followed by an intraperitoneal injection of 1 mCi of [¹⁸F]-FDG. After uptake period (40 min awake), each rat was placed in a headfirst prone position and scanned for 10 min under inhalatorial anesthesia (1.5%–2.5% maintenance dose). All the scans were performed with rats under 12-hr fasting and the body temperature was kept at 36°C. The static radiotracer readings were acquired with the field of view (FOV: 3.75) centered on the rat's head. At the end of the acquisition, rats were returned to their cages until complete recovery.

Data were reconstructed by the maximum likelihood estimation method (MLEM-3D) algorithm with 20 iterations. Each image was reconstructed and spatially normalized into a [¹⁸F]-FDG template using brain normalization in PMOD v3.5 and the Fusion Toolbox (PMOD Technologies, Zurich, Switzerland). The rat brain template for MRI was used to overlay the normalized microPET images. Glucose metabolism was normalized for the injected dose and animal body-weight and, expressed as standard uptake values (SUVs). SUVs of 58 brain regions (26 bilateral and 6 unilateral) were extracted using a predefined volumes of interest (VOI) template. Moreover, SUVs of all brain regions were normalized by the pons and expressed as relative standardized uptake value (SUVr). Further analyses were conducted by MINC tools (www.bic.mni.mcgill.ca/ServicesSoftware) (Nunes Azevedo et al. 2020).

Metabolic brain networks (MBN), derived from [¹⁸F]-FDG SUV regional data, were constructed by computing Pearson's correlation coefficient based on 1,000 bootstrap samples. The correlation maps were built using 12 VOIs: left (L)-right(R) L-R striatum, L-R frontal cortex, L-R parietal cortex, L-R hippocampus, L-R, cerebellum, and L-R thalamus. Graph theoretical measures such as global efficiency, density, assortativity coefficient, average degree, and average clustering coefficient were computed using 10 MBNs most similar to group mean MBN. In short, global efficiency is a measure of how effectively the network interchange information between its nodes; density quantifies the overall number of edges of a network; assortativity coefficient measures the network resilience; average degree refers to the number of connections a node of a graph has with other nodes, and the clustering coefficient corresponds to the portion of the node's neighbors that are also neighbors of each other (Rubinov & Sporns, 2010). MBNs were corrected for multiple comparisons using false discovery rate (FDR) at $p < .001$ (Bellaver et al., 2019; Zanirati et al., 2018).

2.4 | Cognitive function assessment

Spatial memory was assessed from PND 65 to 70 by means of the MWM test, according to a previous protocol (Netto et al., 1993). During the training period, the platform was placed in one of four quadrants of the pool and kept in the same position over the days. Each rat was placed into the water facing the wall at one of the four start positions. The animal was removed from the pool when it found the platform and the latency was recorded. In case it did not find the platform after 60s of swimming, it was gently guided and placed on the platform for additional 20s. Rats received four trials per day, with an inter-trial interval of 10 min. for five training days. On the sixth day the probe trial was performed; the platform was removed from the pool and each rat was placed into the water on the diagonally opposite side of the platform, allowing it to swim freely for 1 min before it withdrew from the water. The movement was tracked, and the animal's behavior was evaluated using the software ANY-maze™. Swimming strategies were labeled by three evaluators, according to the six classes previously described (Higaki et al., 2018;

Illouz et al., 2016): (a) Thigmotaxis: animal swims close to the pool walls, spending more time in the periphery zone; (b) Passive: animal explores a limited area of the pool; (c) Random: swim trajectories show a wide and repeated search around the pool, as well as sudden changes in direction without any circular pattern; (d) Circling: animal explores the pool away from the walls, often drawing a circular trajectory around the pool; (e) Focused-search circling: animal swims mainly within two quadrants of the pool, including the platform zone; and (f) Focused search: animal swims straight from the starting point to the platform zone, showing an exploration strategy focused on the correct area. The performance of each probe trial was then scored using as reference a previous study, according to the following scale: thigmotaxis: 1; passivity: 1; random: 2; circling: 3; focused-search circling: 5; and focused search: 6. The cognitive score of each animal was normalized to 6, which is the highest score possible (Illouz et al., 2016).

2.5 | Biochemical analysis

On PND 72 brains were quickly collected following decapitation. The right hippocampus (ipsilateral to the carotid occlusion) was dissected out and immediately frozen in liquid nitrogen and stored at -80°C until analysis. Samples were homogenized in a 10 mM Hepes buffer and 1% protease inhibitor cocktail (Cat. No. 11,697,498,001, Roche, Germany) with pH: 7.9. To enrich the homogenates with membrane proteins, detergents were added to the extraction buffer (Seddon et al., 2004). We used both a non-ionic detergent (1% non-idet P-40 substitute, Cat. No. 9016-45-9; Sigma-Aldrich), which disrupts membrane structure, but does not significantly interfere with subsequent electrophoresis, and an ionic bile-acid detergent at low concentration (0.25% sodium deoxycholate/ Cat. No. 302-95-4, (D6750); Sigma-Aldrich). Sodium deoxycholate has been shown to facilitate transmembrane protein extraction, solubilization, and stability in aqueous solution (Odahara, 2004; Zhou et al., 2006). Tissue extracts were centrifuged at 960 g, for 10 min, at 4°C and supernatants were collected. Total protein content was calculated using the PierceTM BCA Protein Assay kit (Cat. No. 23225; Thermo-Fisher Scientific). Equal protein concentration (40 μg of total protein/lane) was loaded in 4%–12% gradient polyacrylamide gels (Cat. No. NP0323BOX; Thermo-Fisher Scientific), together with a 12–225 kDa molecular weight marker (Cat. No. RPN800E; GE Healthcare).

After electrophoresis, proteins were transferred to a nitrocellulose membrane and then blocked for 2 hr in Tris-buffered saline containing tween 20 (T-TBS) and 5% non-fat dry milk. Blots were incubated overnight (4°C) with one of the following antibodies: anti-monocarboxylic acid transporter 4 (MCT4, Cat. No. SC-50329, 1:1,000; Santa Cruz), anti-glucose transporter 1 (GLUT1, Cat. No. ab15309, 1:1,000; Abcam), anti-glucose transporter 3 (GLUT3, Cat. No. ab15311, 1:1,000; Abcam), and anti-glyceraldehyde-3-Phosphate Dehydrogenase (GAPDH, Cat. No. MAB-374, 1:2000; Merckmillipore). GAPDH was used as a loading control. Secondary peroxidase-conjugated anti-rabbit (AP132P, 1:1,000;

Merckmillipore) or anti-mouse antibody (Cat. No. 402335, 1:1,000; Merckmillipore) was incubated for 2 hr at room temperature (23°C) Chemiluminescence signals were detected in an Image Quant LAS4010 system (GE Healthcare) using a PierceTM ECL western Kit (Cat. No. 32106; Thermo-Fisher) (Couto-Pereira et al., 2019).

Average optical density was determined using the software Image Studio Lite (version 5.2). Numeric sample identifiers were used during sample handling. Results were quantified as the ratio between the optical density of the interest protein and the loading control (GAPDH) in the same blot. The absolute optical density of the GAPDH protein was tested in all experiments for differences between groups and was accepted when no significant differences were found. Data are expressed as a percentage of the control group (Sham_SC-SC).

2.6 | Morphological analysis

Rats were deeply anesthetized with isoflurane and then submitted to transthoracic cardiac perfusion with 0.9% NaCl followed by 4% paraformaldehyde in 0.1 M phosphate-buffered (PB). Brains were removed from the skull, placed in 15% sucrose solution for 48 hr, followed by 30% sucrose solution until the brain sank to the bottom of the tube, and then, cryoprotected. Serial coronal 25 μm sections were cut (between 1.00 and 4.52 mm from the bregma) with a Leica CM1850 cryostat at -20°C . Each 10th section was placed in a gelatin-coated glass slide and stored at -20°C until processing. After hematoxylin and eosin (H&E) staining (Cat. No. 517-28-2 and Cat. No. 17372-87-1, respectively; Sigma-Aldrich), brain areas (hemisphere, cortex, hippocampus, and striatum) were outlined manually using NIH-ImageJ software and the relative volumes of ipsilateral and contralateral side to the carotid occlusion were estimated using the following equation: Σ (area of slices) \times (inter-slice interval). Data are expressed as the ratio of ipsilateral to contralateral areas, calculated by the equation: ipsilateral volume (mm^3)/contralateral volume (mm^3), and it was taken as an index of tissue damage caused by HI (Durán-Carabali et al., 2017; Fan et al., 2013).

2.7 | Immunofluorescence analysis

Four serial coronal slices of 25 μm were cut using a cryostat and mounted on glass slides for immunofluorescence analysis. An inter-slice interval of 250 μm was used. Tissue slices were permeabilized with 0.25% Triton-x-100 in phosphate-buffered saline (PBS) for 10 min, and then, blocked with 3% goat serum (Cat. No. G9023; Sigma-Aldrich) for 30 min at 23°C . The slices were incubated overnight with anti-APP (Cat. No. A8717, 1:250; Sigma-Aldrich) and anti-GAP-43 (Cat. No. G9264, 1:200; Sigma-Aldrich) at 4°C . After five times washing in PBS, slices were incubated for 1 hr at 23°C with secondary antibodies conjugate with Alexa fluor 555 anti-rabbit (Cat. No. A-21428, 1:500; Thermo-Fisher) or Alexa fluor 488 anti-mouse (Cat. No. A-11001, 1:500; Thermo-Fisher). Slices were mounted on Fluoroshield



with 4',6'-diamino-2-phenylindole-DAPI (Cat. No. 10236276001; Sigma-Aldrich) and coverslipped. The primary antibody was omitted for immunostaining-negative control reactions. Immunofluorescence in the CA1 region of the hippocampus and parietal cortex was photographed by means of a Nikon E600 microscope. A region of interest was used on each slice and fluorescence intensity was quantified using NIH-ImageJ software (version 1.8.0_112).

2.8 | Statistical analysis

Statistical analysis was performed using the SPSS 21 software. Data normality distribution was tested using the Kolmogorov–Smirnov test, which showed a non-parametric profile for the variables: glucose metabolism, brain tissue volumes, behavioral response during the MWM probe trial and GLUTs levels. Parametric distribution was observed in graph measures of the MBN, MWM training sections latencies, MCT levels, APP and GAP-43 level. Non-parametric data were analyzed using Kruskal–Wallis test followed by Dunn's for multiple comparison test to determine significant differences between experimental groups. Parametric data were analyzed using two-way analysis of variance (ANOVA) followed by Tukey *post hoc* test to compare the main effects of housing condition and HI and the interaction of these factors. The MWM training sessions were analyzed by means of repeated-measures ANOVA. Correlations between histological and metabolic data, as well as between behavioral parameters of the MWM probe trial were calculated by Spearman coefficients. No test for outlier results was conducted and no data was excluded from the analysis. The number of animals required for each experiment was estimated based on previous experience of authors and data available in the literature using a similar methodology (Bellaver et al., 2019; Couto-Pereira et al., 2019; Odorczyk et al., 2020). Thereby, it was estimated that 10–14 animals of each group would be adequate for behavioral assessment and 6–10 animals for the other parameters (metabolism, biochemical, and morphological studies), in order to achieve the power of 80% and significance of $p < .05$. The results are presented as mean and standard error (mean \pm SE). The graphs were plotted using Graph Pad Prism.

3 | RESULTS

3.1 | In vivo glucose metabolism in adult rats' brains after neonatal HI and the effects of early EC on metabolic parameters

Glucose consumption assessed by [18 F]-FDG SUVR showed long-term changes in the brain metabolism of animals submitted to HI and exposed to EC. The average [18 F]-FDG SUVR values for sham and all HI groups are presented in Figure 2a. The analysis of whole brain [18 F]-FDG showed a trend toward lower SUVR levels in the HI_SC-SC group when compared with the sham_SC-SC group ($X^2_{(7)} = 12.880$, $p = .075$ —Figure 2b). Furthermore, neonatal HI caused a significant reduction in ipsi/contralateral ratio of [18 F]-FDG uptake in cerebral

cortex ($X^2_{(7)} = 28.217$, $p = .0001$), hippocampus ($X^2_{(7)} = 25.098$, $p = .0001$), and striatum ($X^2_{(7)} = 32.205$, $p = .0001$). This effect was not observed either in HI animals exposed to neither prenatal or early postnatal EC (Figure 2c–e), suggesting a protective effect of enrichment. No significant differences were observed in the cerebellum (Figure 2f). [18 F]-FDG ipsi/contralateral ratio for all other brain structures analyzed are presented in Table S1.

Figure 2g depicts the percentage of change in the glucose metabolism between sham and HI groups, while Figure 2h shows the percentage of change between HI groups exposed to EC as compared to the HI_SC-SC group. The HI_SC-SC group showed a reduction of ~11% in brain metabolism (considering the sum of all SUVR brain regions) compared to its respective sham group ($X^2_{(4)} = 10.346$, $p = .035$ —Figure 2i). Moreover, the HI_SC-SC group showed a metabolic reduction of ~30%–40% in the cerebral cortex ($X^2_{(4)} = 27.902$, $p = .0001$), hippocampus ($X^2_{(4)} = 24.872$, $p = .0001$) and striatum ($X^2_{(4)} = 36.996$, $p = .0001$), confirming a well-described regional vulnerability to HI insult. Conversely, HI animals exposed to early EC show less features of metabolic decline (from 7% to 15%) compared to the HI_SC-SC group (a range from 11% to 40%), as presented in Figure 2j–l. However, animals of the HI_EC-EC also exhibited a reduction in glucose metabolism in the cerebral cortex when compared with the sham group (Figure 2j). No significant differences in glucose metabolism were found in the groups of HI animals exposed to EC either prenatally or postnatally.

3.2 | Patterns of inter-hemispheric metabolic networks following neonatal HI and early EC

Figure 3a,b display the correlation coefficient matrices of sham and HI groups, evidencing that MBN of HI animals presents less statistically significant nodes, with the ipsilateral hemisphere to carotid occlusion being most affected. An interaction between housing condition and HI procedure was observed in all graph measures, revealing reduced global efficiency ($F_{(3,72)} = 38.76$, $p = .0001$ —Figure 3c), lower density ($F_{(3,72)} = 10.35$, $p = .0001$ —Figure 3d), increased assortativity coefficient ($F_{(3,72)} = 33.48$, $p = .0001$ —Figure 3e), decreased average degree ($F_{(3,72)} = 17.40$, $p = .0001$, Figure 3d), and reduced clustering coefficient ($F_{(3,72)} = 17.70$, $p = .0001$ —Figure 3e) in HI animals when compared with their respective sham group. However, HI animals exposed to early EC (during gestation, lactation, and both neurodevelopmental periods) showed an increase in the network efficiency and reduction in the assortative coefficient when compared with the HI_SC-SC group (Figure 3c,d). In addition, animals of the HI_SC-EC group showed an increase in the clustering coefficient when compared with HI_SC-SC and HI_EC-SC groups. Interestingly, the HI_EC-EC group presented significant improvements in all graph measures when compared with the other HI groups (Figure 3c–g), suggesting that prolonged enrichment during critical periods of the neurodevelopment can have a greater impact in the MBN reorganization following neonatal HI. No significant differences in the MBN assessments were observed between sham groups.

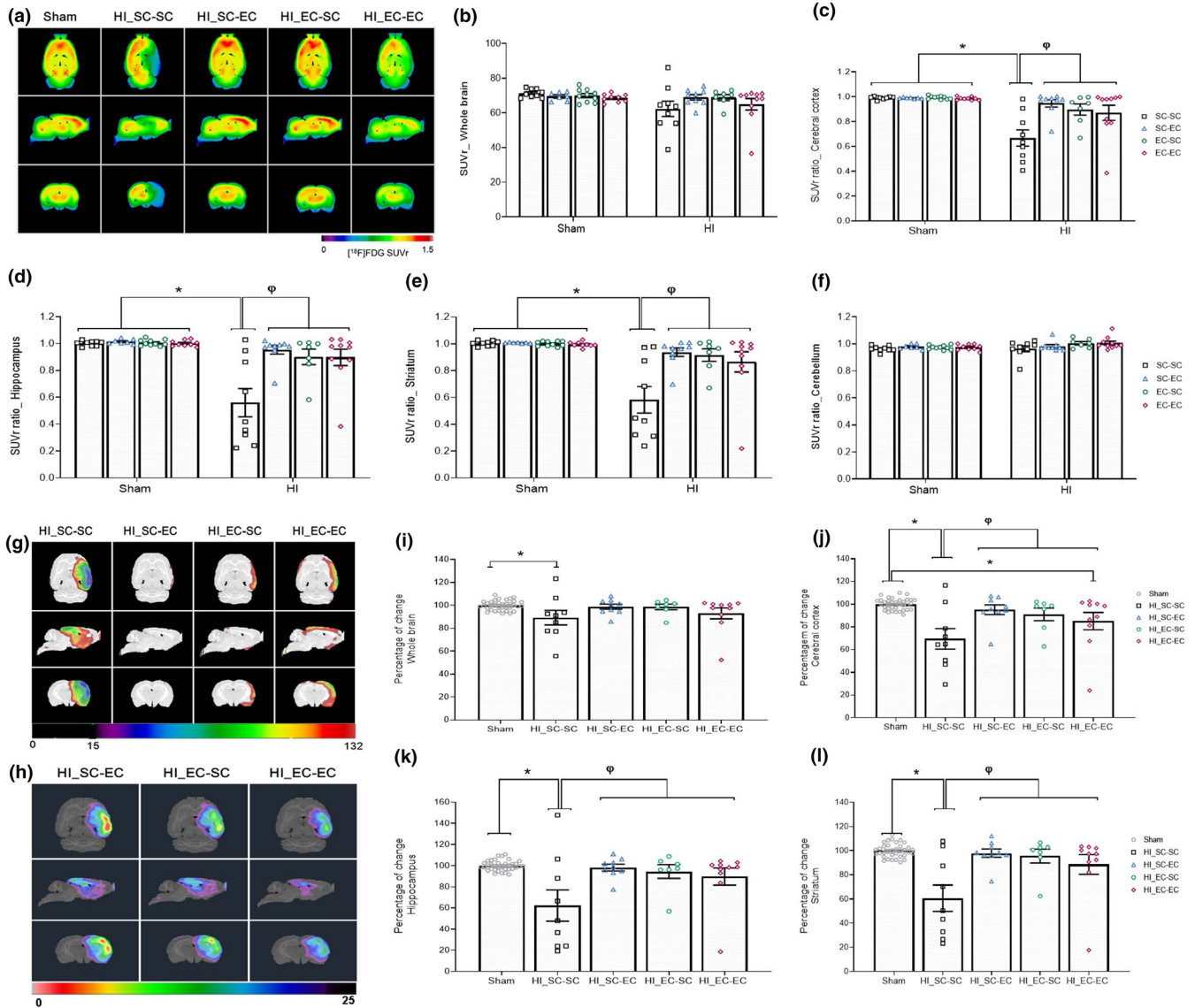


FIGURE 2 Brain glucose metabolism assessment using [^{18}F]-FDG. (a) Average of relative standardized uptake value (SUVr) for [^{18}F]-FDG in sham and HI groups—all brain regions were normalized by the pons. (b) Sum of all SUVr brain regions, denominated as whole brain. SUVr ratio for (c) cerebral cortex; (d) hippocampus; (e) striatum; and (f) cerebellum. Average image of percentage of change between: (g) Sham and HI groups—representing brain hypometabolism and (h) HI_SC-SC and HI animals exposed to EC, showing brain hypermetabolism. Percentage of SUVr change for (i) whole brain; (j) cerebral cortex; (k) hippocampus and (l) striatum. *Significant difference when compared with sham group. ϕ Difference from all HI groups exposed to EC. $n = 7\text{--}10$ rats per group. Significance accepted at $p < .05$ (Kruskal–Wallis test). Data are presented as mean values \pm SE

3.3 | Effects of neonatal HI and EC in the spatial memory of adult rats

Aiming to verify the long-term spatial memory deficit induced by neonatal HI and the protective effect of EC in the cognitive function, the MWM task was performed. Repeated-measures ANOVA showed that all animals presented a decrease in the latency to reach the platform in the course of training, indicating the learning of the task ($F_{(4,452)} = 79.831, p = .0001$). There were HI ($F_{(4,452)} = 2.660, p = .032$) and housing condition effects ($F_{(12,452)} = 1.949, p = .027$), in which significant differences among sham and HI animals suggest that rats exposed to early EC required less time to find the hidden platform.

The analysis of each individual training day revealed that in the fifth training day animals of the HI_SC-SC group had the worst performance compared to all other experimental groups -sham animals and HI rats exposed to EC ($F_{(3,113)} = 2.782, p = .04$), as depicted in Figure 4a. Considering the overall performance of the animals (Figure 4b), a similar pattern was observed in the area under the learning curve ($F_{(3,113)} = 2.719, p = .048$), in which the HI_SC-SC group showed the worst performance compared to all other experimental groups, with no differences among HI animals exposed to early EC.

Performance in the probe trial (sixth testing day—24 hr after the end of the training period) was considered an indicator of the animal's spatial memory retention. Animals of the HI_SC-SC group

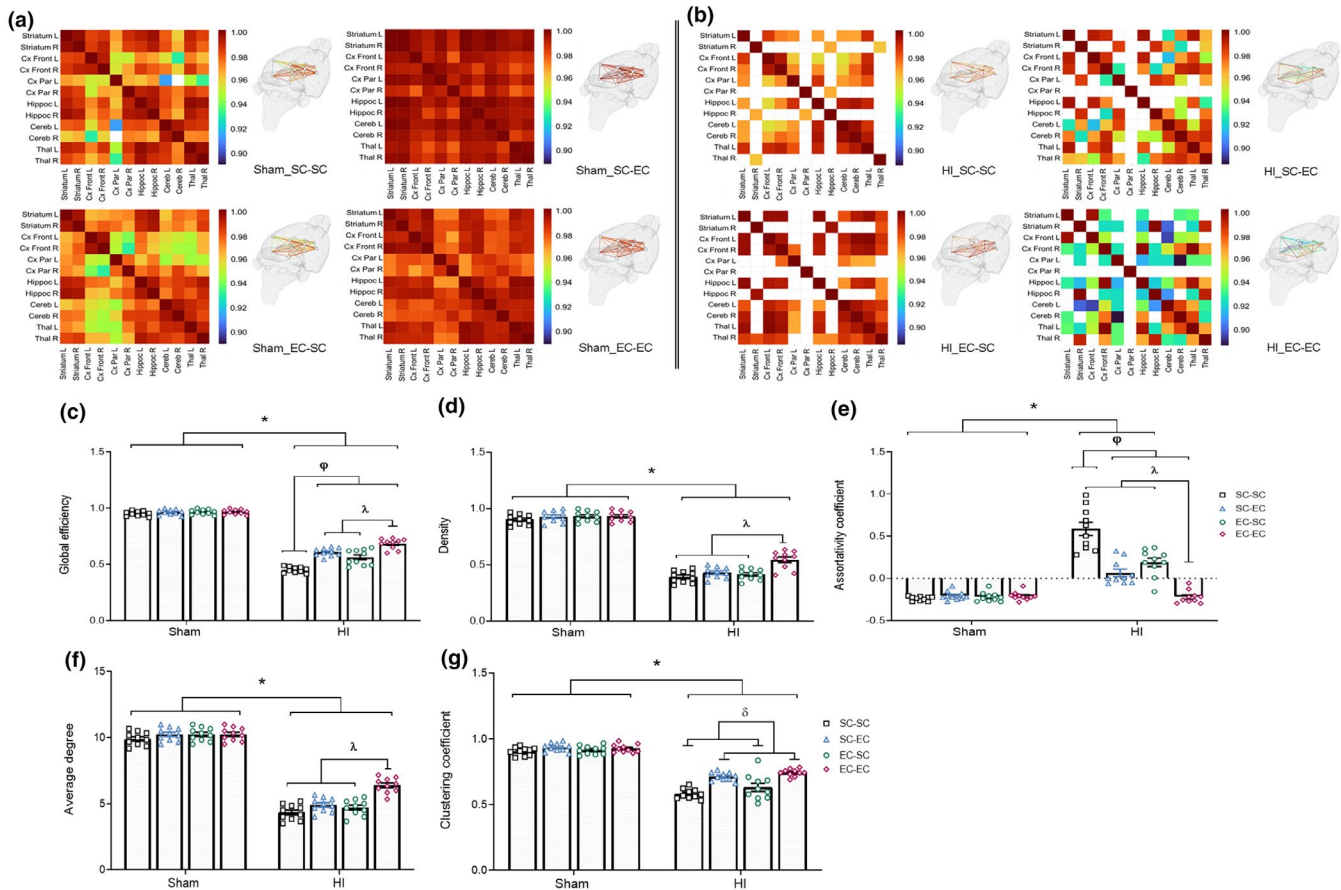


FIGURE 3 Metabolic brain networks derived from [^{18}F]-FDG SUV. Matrices of correlation coefficients between brain regions and 3D brain surfaces displaying metabolic brain network (MBNs) of (a) sham and (b) HI animals of the following groups: SC-SC, SC-EC, EC-SC, and EC-EC. Metabolic network graph measures of (c) global efficiency, (d) density, (e) assortativity coefficient, (f) average degree, and (g) clustering coefficient. Matrices are presented as correlation values with false discovery rate (FDR). Only r -values higher than 0.9 survived after FDR correction (0.9 to 1 from blue to red, respectively). Non-significant correlations are depicted in white. *Significant difference when compared with sham group. ϕ Difference from all HI groups exposed to EC. λ Difference of HI_EC-EC group when compared with other HI groups. δ Difference of HI_SC-EC and HI_EC-EC groups in comparison to HI_SC-SC and HI_EC-SC groups. Significance accepted at $p < .05$ (two-ways ANOVA). Data are presented as mean values \pm SE

showed longer latencies to cross the platform zone as compared to sham groups and HI_EC-SC and HI_EC-EC groups ($X^2_{(7)} = 17.490$, $p = .014$). No significant differences were observed between HI animals exposed to EC as compared to its respective sham group. In addition, a trend to positive behavioral effects was observed in sham groups exposed to EC when compared with sham_SC-SC group ($p = .072$ —Figure 4c). The analysis of time spent in the target quadrant showed that HI_SC-SC animals spent less time in this area when compared with all other experimental groups ($X^2_{(7)} = 17.275$, $p = .016$). This result suggests that spatial memory of animals submitted to HI was improved by early enrichment experiences (Figure 4d). Similarly, there was a reduction in the central zone exploration by the HI_SC-SC compared to the other experimental groups, as observed in Figure 4e.

The analysis of the swimming strategies in the probe trial indicated that rats in the EC displayed a spatial memory enhancement, whereas the HI_SC-SC group had the lowest score when compared with all other groups ($X^2_{(7)} = 23.697$, $p = .001$), as shown in Figure 4f–h and Table S2. A significant difference was observed between the

HI_SC-EC group and its respective sham group. In addition, a trend was found between sham_SC-EC and sham_SC-SC groups ($p = .069$), suggesting that postnatal enrichment could improve hippocampus-dependent memory in sham animals. A moderate positive correlation was found between the cognitive score and the time spent in the target quadrant (Spearman coefficient: 0.699, $p = .001$), suggesting that this parameter could be a better indicator of spatial memory capacity rather than the latency to cross the platform zone for first time in the probe trial (weak correlation—data not shown). Together, these findings indicate an increase in the hippocampus-dependent memory in animals exposed to HI and EC compared to the HI_SC-SC group.

3.4 | Influence of early EC on HI tissue loss and its association with brain [^{18}F]-FDG consumption

Representative H&E-stained histological sections are presented in Figure 5a. HI resulted in a significant reduction of the right hemisphere

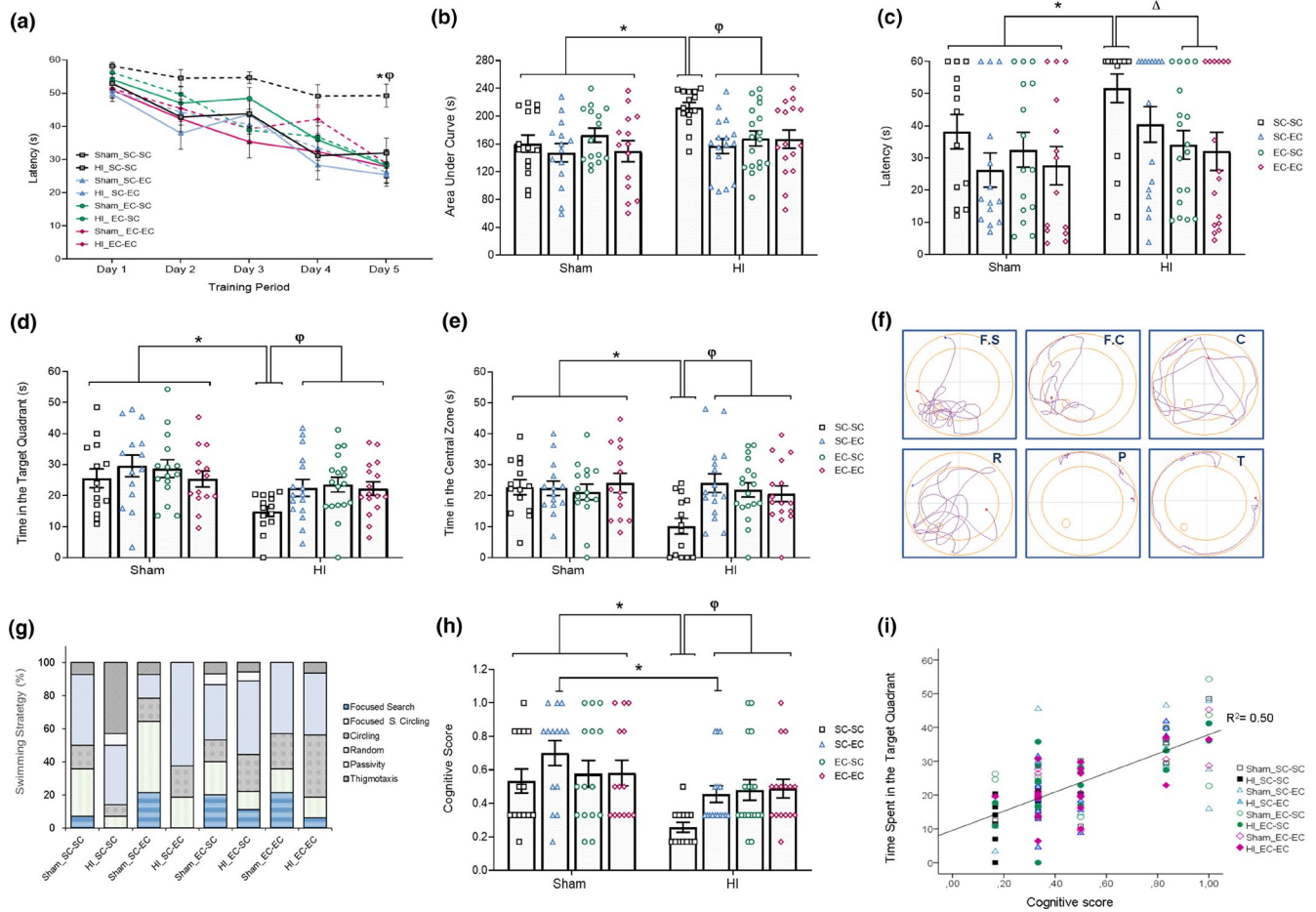


FIGURE 4 Animals performance on Morris water maze task. Training period: (a) latency to find the platform during the training sessions and (b) area under the learning curve during the five consecutive days of training. Probe trial performed 24 hr after the last training day: (c) latency to find the platform; (d) time spent in the target quadrant and (e) time spent in the central zone during the probe trial; (f) represents color-coded percentage of swim strategies; (g) spatial strategy classification during the probe trial; (h) cognitive scores of rats in the probe trial and (i) Scatter plots of Spearman correlation between time spent in the target quadrant and cognitive score. Continuous lines represent sham groups and dotted lines indicate HI groups. Black lines (SC-SC group), blue lines (SC-EC group), green lines (EC-SC group), and red lines (EC-EC groups). *Significant difference when compared with sham group. Φ Difference from all HI groups exposed to EC. Δ Differences between HI_EC-EE and EC-EC groups compared to HI_SC-SC group. $n = 14$ – 17 rats per group. Significance accepted at $p < .05$ (Repeated measures ANOVA and Kruskal–Wallis test). Data are presented as mean values \pm SE. F.S: focused search, F.C: focused search circling, C: circling, R: random, P: passivity, and T: thigmotaxis

volume in the HI_SC-SC group ($X^2_{(7)} = 19.902$, $p = .006$), as depicted in Figure 5b. This effect was less evident in animals exposed to EC during prenatal and early postnatal period. A similar pattern was also observed in the cerebral cortex ($X^2_{(7)} = 21.181$, $p = .004$ —Figure 5c) and striatum ($X^2_{(7)} = 20.225$, $p = .005$ —Figure 5d). Interestingly, HI_SC-EC and HI_EC-SC groups showed higher tissue preservation compared to the HI_SC-SC. As depicted in Figure 5e, a significant decrease in the hippocampal volume ratio was observed in the HI_SC-SC group when compared with all other groups ($X^2_{(7)} = 15.364$, $p = .032$). Altogether, these findings revealed that the brain tissue loss in the HI_SC-SC group was between 43% and 52%, whereas in the HI groups exposed to EC it was between 8% and 28%, suggesting that enrichment during early neurodevelopmental periods reduce the tissue damage after HI. Moreover, Spearman correlation analysis showed that the SUVr in the cerebral cortex ($r = 0.906$, $p = .0001$),

hippocampus ($r = 0.849$, $p = .004$), and striatum ($r = 0.895$, $p = .0001$) had a strong positive correlation with the volume ratio of each structure (Figure 5f,g). These data indicated that the tissue preserved by EC exhibits active metabolic responses.

3.5 | Effect of neonatal HI and early enriched exposure on hippocampal transport protein levels in adulthood

The analysis of GLUT in the right hippocampus showed a reduction in GLUT1(55kDa isoform) levels in the HI_SC-SC group compared to its respective sham group ($X^2_{(7)} = 14.047$, $p = .050$), as depicted in Figure 6a. Furthermore, there was an increase in the second isoform of GLUT1 (42 kDa) in the hippocampus of rats from the EC-EC group (sham and HI)

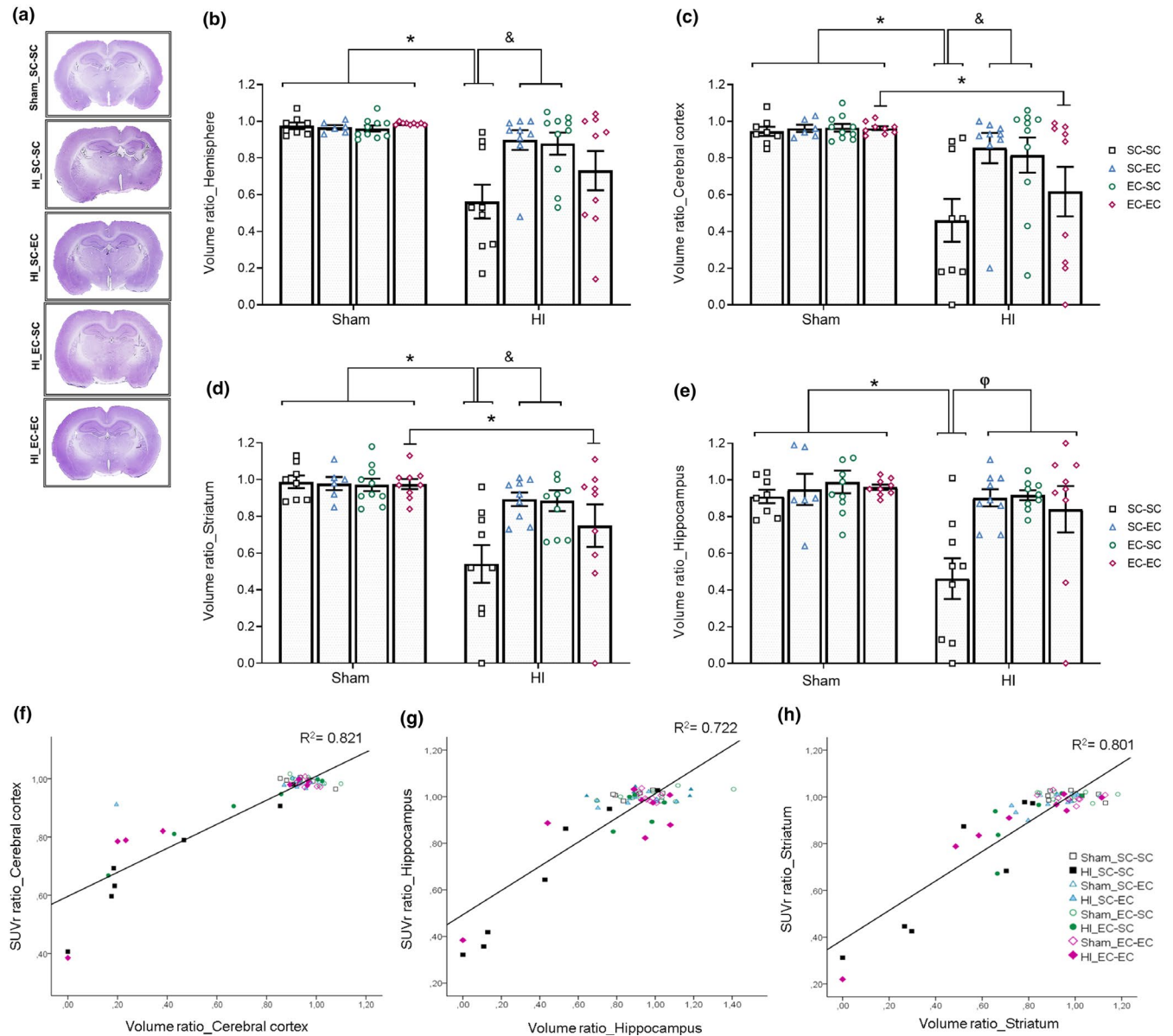


FIGURE 5 Brain hemispheres and selected structures volume ratios. (a) Representative image of each experimental group using hematoxylin and eosin staining; (b) hemisphere; (c) cerebral cortex; (d) striatum and (e) hippocampus volume ratio. Scatter plots of Spearman correlation analysis between SUVR and volume ratio of (f) cerebral cortex; (g) hippocampus and (h) striatum. *Significant difference when compared with sham group. ϕ Difference from all HI groups exposed to EC. &Differences between HI_SC-EC and EC-SC group compared to HI_SC-SC group. $n = 6-10$ rats per group. Significance accepted at $p < .05$ (Kruskal–Wallis test). Data are presented as mean values \pm SE

when compared with the SC-SC group ($\chi^2_{(7)} = 14.086, p = .05$). No significant differences were observed between SC-EC and EC-SC groups (Figure 6b). Both GLUT3 and MCT4 levels did not differ significantly among groups when evaluated at adulthood ($p > .05$ —Figure 6c,d).

3.6 | Long-term levels of proteins related to neuroplasticity in rats that underwent HI is altered by early EC

Representative images of the levels of APP in the cerebral cortex and the hippocampus are shown in Figure 7e,f. A substantial increase

in the intensity of fluorescence in the CA1 area of the hippocampus (~2 folds) in the HI_SC-SC group was observed ($F_{(3,41)} = 4.795, p = .006$ —Figure 7a). Similarly, higher APP fluorescence intensity was observed in the cerebral cortex of the HI_SC-SC group ($F_{(3,43)} = 8.674, p = .0001$ —Figure 7b). There were no significant changes in the ipsi/contralateral ratio of the evaluated areas, indicating that animals of the HI_SC-SC group exhibited an increase in APP levels on both hemispheres at adulthood, and this effect was not observed in animals exposed to EC (Figure 7c,d).

The analysis of GAP-43 levels did not reveal significant changes both in the hippocampus and cerebral cortex when each hemisphere was considered. Nevertheless, an injury effect was observed

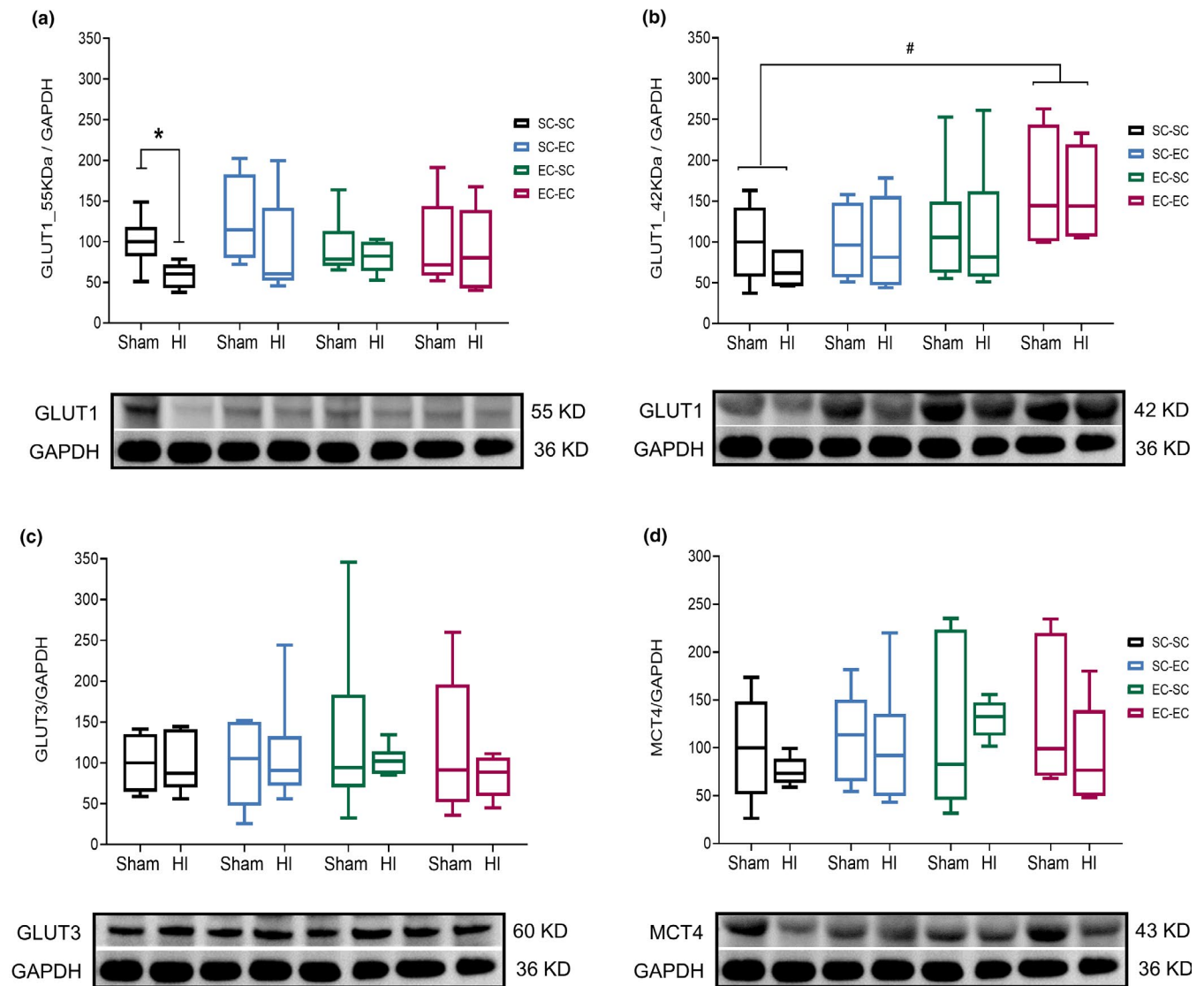


FIGURE 6 Protein levels of GLUT and MCT4 in the right hippocampus. Quantification of (a) 55kDa isoform of GLUT1; (b) 42kDa isoform of GLUT1 (c) GLUT3 and (d) MCT4. Representative blots of each protein are presented under each chart. Median values are indicated by the central mark and 25%–75% percentiles are shown by box edges. *Significant difference when compared with sham group. #Difference between animals enriched during prenatal and lactation period (EC-EC group) compared to control group (SC-SC). $n = 4-9$ rats per group. Significance accepted $p < .05$ (Kruskal-Wallis test)

in the ipsi/contralateral ratio of GAP-43 in the cerebral cortex ($F_{(1,44)} = 7.425$, $p = .009$), evidencing a reduction of protein levels in the HI_SC-SC group when compared with its respective sham group (Figure 8b,c). Moreover, a housing condition effect was found in the ratio of GAP-43 content in the hippocampus ($F_{(3,40)} = 3.843$, $p = .017$ —Figure 8a), indicating that animals exposed to EC during the prenatal period (EC-SC group) had an increase in GAP-43 levels as compared to the EC-EC group.

4 | DISCUSSION

This study showed long-term changes in brain glucose metabolism and MBNs architecture in adult rats that received neonatal HI

at PND 3. Analysis of [^{18}F]-FDG microPET images evidenced HI-induced brain hypometabolism, especially in regions with higher metabolic demands such as cerebral cortex, hippocampus, and striatum, as well as a reduction in MBN synchrony and glucose transporter levels. Changes in proteins related to axonal plasticity and adult-onset neurodegenerative processes as APP and GAD-43 were also described. Confirming the working hypothesis, it was shown that EC during sensitive periods of the neurodevelopment (gestation and lactation period) reduces glucose metabolic failure, suggesting that the early life environment is able to promote long-lasting metabolic and cellular adaptations, as well as to prevent spatial memory deficits following HI.

[^{18}F]-FDG microPET is a well-established imaging technique to assess changes in glucose brain metabolism. Cerebral HI leads to

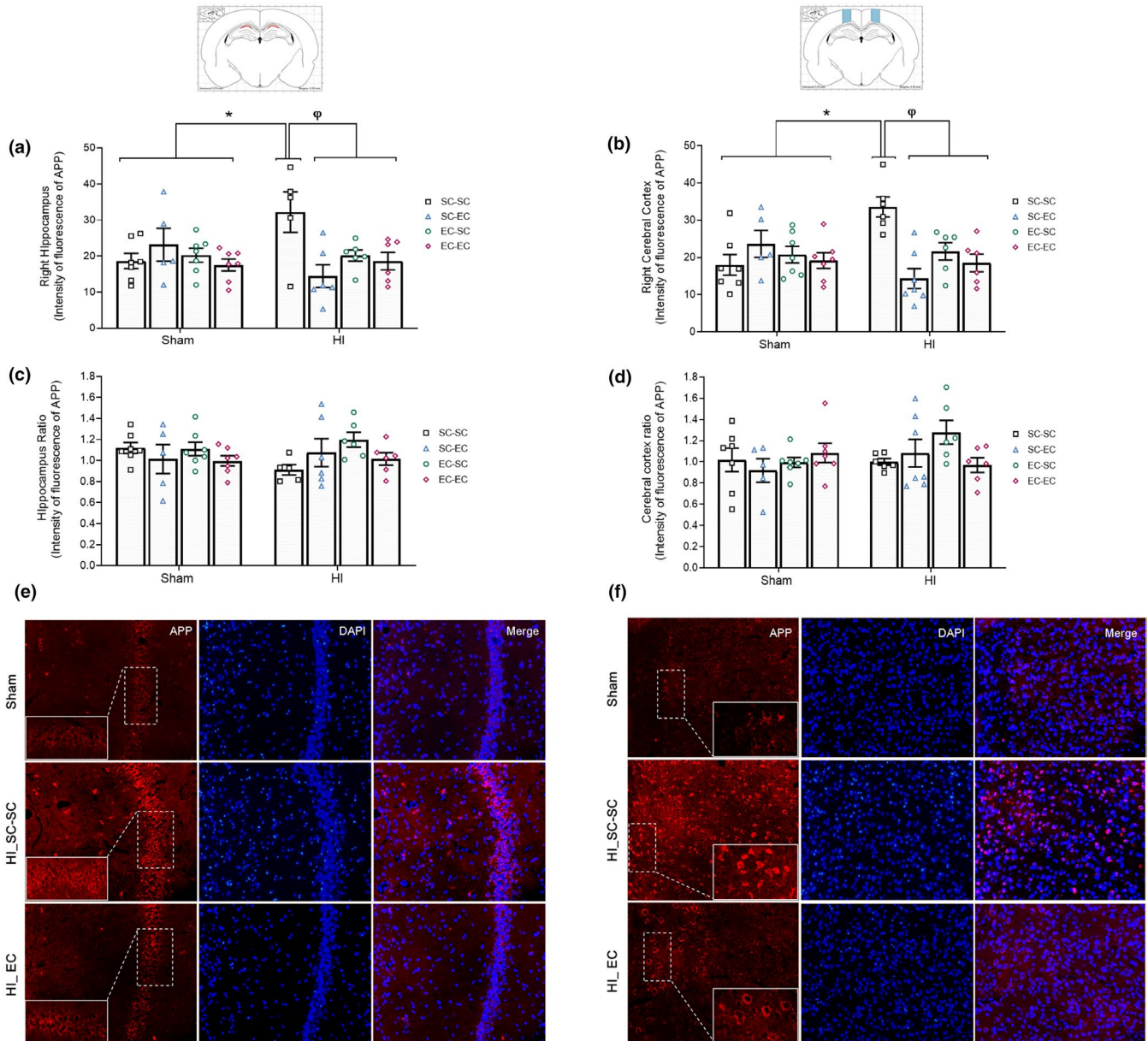


FIGURE 7 Levels of amyloid precursor protein—APP. Fluorescence intensity in: (a) right CA1 region of the hippocampus and (b) right parietal cortex of adult rats submitted to neonatal HI and EC. Ipsi/contralateral ratio of immunofluorescence intensity on (c) CA1 region and (d) parietal cortex. Representative photomicrographs, 20x magnification of hippocampus (e) and cerebral cortex (f). *Significant difference when compared with sham group. ϕ Difference from all HI groups exposed to ECn = 5–7 rats per group. Significance accepted at $p < .05$ (two-way ANOVA). Data are presented as mean values \pm SE

lower glucose availability in the hemisphere ipsilateral to the carotid occlusion during acute stages of the brain insult (Martin et al., 2009). Moreover, this metabolic response displays a negative correlation with injury severity, and the degree of hypometabolism is a predictor of tissue damage (Shi et al., 2012; Thorngren-Jerneck et al., 2001; Zhao et al., 1997). The outcomes of this study showed a long-term reduction in the [18 F]-FDG in the HI_SC-SC group in brain regions like hippocampus, cerebral cortex and, striatum, among others (Figure 2 and Table S1), structures that are most vulnerable to neonatal HI and that are important for cognitive function (Odozycyk et al., 2020). [18 F]-FDG is an indirect measure of synaptic function and reduced

values are associated with impairment of neuronal activity (Torjigan et al., 2016). Thereby, it is suggested that early brain insult may increase the risk of impairments in brain glucose metabolism as well as the development of progressive neurodegeneration in the adult brain (Martin et al., 2019; Cunnane et al., 2012; Jack et al. 2018).

The EC before (prenatal) and after (lactation) neonatal HI was able to preserve in vivo brain metabolism, even when the pups were exposed to the enrichment in different neurodevelopmental periods (during intrauterine life or after birth). The attenuation of glucose hypometabolism in animals exposed to EC, could imply differences in compensatory mechanisms during or after HI, considering

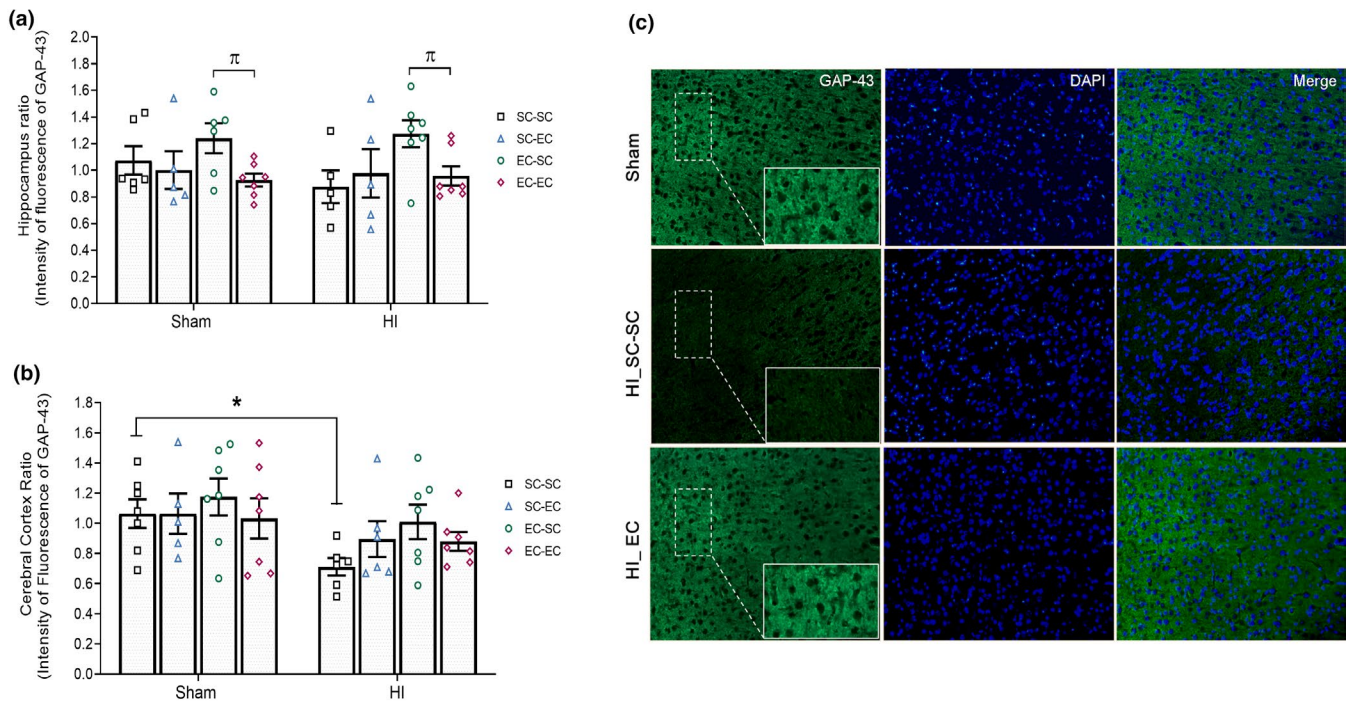


FIGURE 8 Levels of growth-associated protein—GAP-43. Ipsi/contralateral ratio of immunofluorescence intensity of (a) CA1 region and (b) parietal cortex. (c) Representative photomicrographs, 20x magnification on cerebral cortex. *Significant difference when compared with sham group, π Difference from prenatal EC (EC-SC group) compared to EC-EC group. $n = 5-7$ rats per group. Significance accepted at $p < .05$ (two-way ANOVA). Data are presented as mean values \pm SE

physiological characteristics in the use of energy substrates in the neonatal period, as well as the degree of maturation of glutamatergic receptors and glucose transporters (Brekke et al., 2014), factors that can determine the injury pattern (Brekke et al., 2017). Furthermore, prenatal and postnatal manipulations may involve modulation of gene and protein expressions later in adult life. With the use of proteomics analysis, Kang and colleagues reported that environmental enrichment beginning in the prenatal and early postnatal period reduced the levels of protein implicated in energy metabolism (Kang et al., 2016). However, the contents of these proteins were not evaluated, and further studies are needed to elucidate whether both periods share similar mechanisms in the regulation of cerebral metabolism, or if they activate different molecular pathways.

Cellular modifications induced by EC express the intrinsic capacity of the CNS to compensate for structural damage and to facilitate post-injury functional recovery (Dennis et al., 2013). Neonatal HI at PND 3 caused a significant volume reduction in different brain regions of the HI_SC-SC group. This tissue loss is similar to previous literature reports, which have also described an association with behavioral impairments (Alexander et al., 2014; Durán-Carabali et al., 2019; Sanches et al., 2013). Despite the vulnerability of the cerebral cortex, striatum, and hippocampus to HI insult, EC during prenatal, and lactation period allowed that preserved tissue maintained an active metabolic response, as observed in HI_EC-SC, HI_SC-EC and HI_EC-EC groups (Figure 5). The preservation of metabolically active brain tissue could be important during recovery processes based on two aspects: first, compensatory mechanisms may not be limited to optimizing neuronal circuits in uninjured brain regions;

secondly, the metabolic response allows for better cellular reorganization in the tissue affected by the HI event (Grefkes & Ward, 2014). It is plausible that the improvement in each time point would implicate different and convergent mechanisms. Interestingly, the continuous enrichment did not confer additional structural and functional improvements in animals suffering neonatal HI, being in accordance with previous reports (Durán-Carabali et al., 2019; Koo et al., 2003). Moreover, a subtle reduction of its positive effect on morphological parameters was observed in the HI_EC-EC group (Figure 5). That draws attention to the need of refining the duration of enrichment protocols at critical neurodevelopmental periods, which could also require the presence of resting periods to modulate recovery processes in rats suffering neonatal HI.

Brain glucose utilization is directly proportional to synaptic activity (Sokoloff, 1993; Zimmer et al., 2017). The coupling between synaptic activity and glucose metabolism allows for the identification of MBN using inter-subject cerebral [18 F]-FDG regional values (Chugani et al., 1987; Zimmer et al., 2017). Hence, MBNs provide information about the energetic architecture of the brain, revealing which regions are working in a synchronous fashion. In this study, a decrease in MBN synchrony was observed after neonatal HI (Figure 3). Reduction in global efficiency, network density, and average degree is related to loss of brain capacity for parallel information exchange and integrative processing (Berlot et al., 2016). The decrease in the clustering coefficient suggests functional changes in segregated synaptic processes as consequences of the lower interconnection of a group of brain regions (Berlot et al., 2016; Rubinov & Sporns, 2010). Moreover, neonatal HI increases the assortativity



coefficient, indicating a possible compensatory mechanism through a core of jointly interconnected nodes, in an attempt to increase MBN resilience (Rubinov & Sporns, 2010). Research using different experimental models such as epilepsy (Zanirati et al., 2018), sepsis (Bellaver et al., 2019), as well as clinical research on adult-onset neurodegenerative diseases (Horwitz et al., 1987; Huang et al., 2018) reported a reduction in MBN connection as an indicator of metabolic brain architecture disruption.

A recent study using the HI model at PND7 demonstrated changes in the architecture of MBN even in the absence of significant glucose hypometabolism (Nunes Azevedo et al. 2020), which is in concordance with outcomes observed in animals exposed to EC. In spite that early EC did not protect against the uncoupling between brain regions induced by HI, the MBN remodeling after neonatal insult could be critical to mediate recovery mechanisms. Thereby, changes induced by EC in the MBN of HI animals could reflect decreased tissue damage and would explain EC effects on behavioral performance. Present results showed that following neonatal HI, global properties of the MBN could be modulated by early EC especially when stimuli are continuously presented during critical stages of the neurodevelopment. Although it has been shown that HI induces several effects in synaptic function, the knowledge about the underlying MBN and how EC may change them is sparse. Additional research testing other VOIs and age-dependent effects on MBN would help to determine the characteristics of MBNs in neonatal models of HI. Furthermore, MBN analyses should be tested in observational clinical studies since they may hold promise as a predictor of cognitive outcomes.

Cognitive deficits, especially in hippocampal-based spatial memory tasks are consistently described in the literature as consequences of neonatal HI (Fan et al., 2005; Huang et al., 2009; Netto et al., 2017; Waddell et al., 2016). In line with previous results, a reversal of HI-induced memory impairment was observed using the same enriched protocol (Durán-Carabali et al., 2017, 2019). In fact, animals exposed to EC showed similar outcomes to the control group (Sham_SC-SC), spending more time in the target quadrant during the probe, indicating an improvement in both learning and spatial memory. In order to explore the effects of EC in the hippocampus-dependent memory of HI animals in more detail, the analysis of swimming strategy of the probe trial was performed (Figure 4 and Table S2). Thigmotaxis swim is generally used as an index of anxiety (Treit & Fundytus 1988) and reflects the animals' difficulties in problem solving (Vorhees & Williams, 2006). Data evidenced that EC reduced thigmotaxis and increased focused-search circling and circling strategies, reflecting a more adaptive approach to locate the platform (Sparling et al., 2010) and reduction in the exploration process disturbance, leading to a better cognitive score. Enriched experiences seem to be a hippocampus-dependent memory enhancer in subjects suffering neonatal insults. This effect could be influenced by the degree of CNS maturation, considering the brain growth spurt phases (Sale et al. 2014; Sale, 2018), allowing more plastic processes and greater susceptibility to external stimuli in order to promote adequate brain maturation, organization, and function (Nithianantharajah and Hannan, 2006).

Brain GLUT and MCT are important for brain metabolism and exhibit also different protein levels from the newborn to the adult (McQuillen et al., 2017). The 55 kDa isoform of GLUT1 is a main protein that facilitates the transport of blood glucose across the BBB, whereas its lighter isoform (42 kDa) ensures glucose delivery to glial cells (McQuillen et al., 2017). GLUT3 is the primary neuronal glucose transporter (Camandola & Mattson, 2017), while MCT4 is exclusively expressed in astrocytes and is present during all stages of development, reaching adult levels at PND 14 (Rafiki et al., 2003). Cerebral maturation enhances glucose utilization as a primary oxidative source through an increase in the concentration of GLUT1 and GLUT3 (McQuillen et al., 2017). The results reported evidence that HI reduced the GLUT1 levels both of 55 kDa and 42 kDa isoforms, in animals of the HI_SC-SC group, with no effects on GLUT 3 levels (Figure 6). Vannucci et al., (1998) demonstrated an increase in GLUT 1 in early (24 hr) and late responses (72 hr) after HI insult at PND 7, as well a loss of GLUT 3 at 72 hr, however, there was no assessment at adulthood. Recent data on GLUT suggest that subtle alterations (~18%) in endothelial and astrocytic GLUT1 deplete neuronal glucose and reduce the tolerance of glial cells (Barros et al., 2017). In addition, some authors suggest that GLUT1 impairments may contribute negatively to brain function more than changes in the specific neuronal transporter (GLUT3) (Barros et al., 2017; Winkler et al., 2015). Thereby, it had been proposed that early repletion of GLUT1 protein could be a pharmacological target in vascular-neuronal dysfunction and GLUT1 deficiency syndromes, improving brain metabolism (Tang et al., 2017; Winkler et al., 2015). We hypothesize that in neonatal HI insult, restoration of GLUT1-isoforms could be an important focus of future studies, in order to reduce brain hypometabolism.

Early EC showed a protective effect mitigating GLUT1 loss, which could be associated with an increase in glucose uptake. Previous studies using environmental enrichment describe that sustained stimulation increases neuronal activity. This causes an increase in microvascular density (determined by GLUT-1 levels) in the cerebral cortex of adult animals (He et al. 2017). A similar result was observed at several ages of development in animals exposed to prenatal EC, indicating that high GLUT1 could be associated with microvascular network reorganization depending on tissue metabolic demand (Argandoña et al., 2005). In this study, animals exposed to EC during prenatal and lactation periods (EC-EC group) showed higher levels of 42kDa isoform of GLUT-1, suggesting the neuroprotective long-term role of astrocytes after HI and that prolonged stimulation is needed to facilitate this response both in healthy subjects and in the ones suffering neonatal HI.

APP plays an important role in the CNS (Hefter et al., 2019) and hypoxic insults can alter protein levels (Nalivaeva et al., 2018; Salminen et al., 2017). An increase in APP levels was observed in the CA1 region of the hippocampus and in the cerebral cortex of the HI_SC-SC group, both in the ipsilateral and contralateral injured hemisphere (Figure 7). This finding is in accordance with Nalivaeva and co-workers who demonstrated an increase in APP levels at different postnatal ages in the sensorimotor cortex after prenatal hypoxia (Nalivaeva et al., 2003). APP increase might

be an index of axonal neuronal lesions (Masliah & Terry, 1993) and may be part of different adaptive synaptic responses after acute neonatal insults such as stroke and hypoxia (Hefter & Draguhn, 2017; Hefter et al., 2016). APP accumulation has been observed in damaged axons and in the early stages of pathologies associated with hypometabolism such as Alzheimer's disease (Stokin & Goldstein, 2006). In addition, high APP levels combined with low GLUT1 levels induced early neurodegeneration, neuronal loss, and behavioral deficits in aged animals (Winkler et al., 2015). Despite some controversies about the impact of higher levels of APP in adult brain function, literature supports the possibility that this protein participates in neuropathological pathways to induce early-onset neurodegenerative diseases (Bhadbhade & Cheng, 2012) or to modulate synaptic changes as consequences of brain dysfunction (Hefter & Draguhn, 2017). HI animals exposed to EC did not exhibit APP increase in analyzed areas. Studies in adult rodents had demonstrated that EC prevented higher APP levels in animals exposed to risk factors to neurodegenerative conditions (Herring et al., 2011; Selvi et al., 2017), keeping values like the control group. This finding is consistent with the data presented here. Further studies are needed to determine whether the protective effects of early EC are mediated by APP regulation.

The neuromodulin GAP-43 is an important neuro-specific protein widely used as a biomarker of cytoskeletal organization, regenerative processes, and growth of the axon terminal, playing an important function in mediating experience-dependent plasticity (Benowitz & Routtenberg, 1997; Holahan et al., 2007). In this study, the HI_SC-SC group showed lower levels of GAP-43 in the cerebral cortex compared to sham group (Figure 8). Literature regarding GAP-43 levels in animals exposed to hypoxia/ischemia is controversial. For instance, in the HI model some authors described higher levels of GAP-43 at different time points (Chen et al., 2012; Sun et al., 2007). Other studies observed up-regulation of this protein in the first weeks after hypoxia with a gradual decrease over time (Zhu et al., 2019) or lower levels after a brain insult (Cai et al., 2012). Moreover, changes in the levels of synaptic proteins such as GAP-43, can suggest adaptive responses in the early stages following hypoxia exposure, in order to maintain cellular homeostasis. Interestingly, reduction of GAP-43 at adulthood in animals exposed to hypoxia insults have been associated with cognitive decline (Zhu et al., 2019) and Alzheimer's disease (Hartl et al., 2008). Animals exposed to EC did not exhibit lower GAP-43 levels in comparison to their respective sham group 63 days after neonatal HI, as observed in the HI_SC-SC group. Some studies have shown that EC causes an increase in GAP-43 achieving levels comparable to the control group under conditions such as permanent middle cerebral artery occlusion (Wang et al., 2019), post-traumatic stress disorder (Golub et al., 2011) and prenatal stress (Zhang et al., 2012). Those previous reports are in accordance with the outcomes presented here. Thereby, enrichment could facilitate the maintenance of GAP-43 levels after neonatal brain insults, participating in synaptic remodeling processes and behavioral responses.

Although the results here presented to confirm the working hypothesis, there are some methodological limitations and the results should be interpreted with caution. The use of male animals did not allow the evaluation of sex dimorphism, while it is recognized that sex influences the HI-induced damage and the efficacy of therapeutic strategies (Netto et al., 2017). Despite the method employed to determine the cognitive score is acceptable for the purpose of screening, the use of an algorithm in the MWM analysis may provide a broader and more accurate index of hippocampus-dependent memory (Illouz et al., 2016). There is a technical limitation in the assessment of brain glucose metabolism using small animals, since, the reduced size of some anatomical structures is close to the spatial resolution limit of the tomograph, making it difficult to determine metric parameters as well as comparisons with clinical data (Chiaravalloti et al. 2019). Furthermore, an intrinsic variability of the extent of brain injury following the experimental HI model has been observed and should be considered (Rumajogee et al., 2016).

Concluding, our findings point out that EC during critical neurodevelopmental periods leave lifelong marks that are important to reduce metabolic dysfunction, to maintain the levels of synaptic proteins as APP and GAP-43 and to improve spatial memory assessed in adulthood rats that received HI at PND 3. To the best of our knowledge, this is the first report providing in vivo evidence as regards the effects of gestational and lactational EC in reducing prolonged metabolic dysregulation, using [18 F]-FDG as a neuronal injury imaging biomarker. These results support the concept that prenatal and early postnatal EC can act as a long-term disease-modifying factor and have a potential translational advantage to reduce brain vulnerability to neonatal HI.

ACKNOWLEDGMENTS

This study was supported by research grants from the Conselho Nacional de Desenvolvimento Científico e Tecnológico (CNPq, Brazil; Chamada Universal MCTI/CNPq No 01/2016, grant number 405470/2016-9) and Coordenação de Aperfeiçoamento de Pessoal de Nível Superior (CAPES). The authors also thank the staff of the Reproduction and Laboratory Animal Research Center from Biochemistry Department-UFRGS.

All experiments were conducted in compliance with the ARRIVE guidelines.

CONFLICT OF INTEREST

The authors declare that they have no conflict of interest.

ORCID

Luz Elena Durán-Carabali  <https://orcid.org/0000-0002-9035-6275>
Natividade de Sá Couto-Pereira  <https://orcid.org/0000-0003-1650-0803>

REFERENCES

- Alexander, M., Garbus, H., Smith, A. L., Rosenkrantz, T. S., & Fitch, R. H. (2014). Behavioral and histological outcomes following neonatal HI injury in a preterm (P3) and term (P7) rodent model. *Behavioral Brain Research*, 259, 85–96.



- Argandoña, E. G., Bengoetxea, H., & Lafuente, J. V. (2005). Lack of experience-mediated differences in the immunohistochemical expression of blood-brain barrier markers (EBA and GluT-1) during the postnatal development of the rat visual cortex. *Developmental Brain Research*, *156*, 158–166.
- Azevedo, P. N., Zanirati, G., Venturin, G. T., Schu, G. G., Durán-Carabali L. E., Odorcyk, F. K., Soares, A. V., de Oliveira Laguna G., Netto, C. A., Zimmer, E. R., & da Costa, J. C. (2020). Long-term changes in metabolic brain network drive memory impairments in rats following neonatal hypoxia-ischemia. *Neurobiology of Learning and Memory*, *171*, 107207.
- Barros, L. F., San, M. A., Ruminot, I., Sandoval, P. Y., Fernández-Moncada, I., Baeza-Lehnert, F., Arce-Molina, R., Contreras-Baeza Y., Cortés-Molina F., Galaz A., Alegría K. (2017). Near-critical GLUT1 and neurodegeneration. *Journal of Neuroscience Research*, *95*, 2267–2274.
- Bayne, K. (2018). Environmental enrichment and mouse models: Current perspectives. *Anim. Model. Exp. Med.*, *1*, 82–90.
- Bellaver, B., Rocha, A. S., Souza, D. G., Leffa, D. T., Bastiani, M. A., De, S. G., Lukaszewicz Ferreira, F. P. C., Venturin, G. T., Greggio, S., Ribeiro, C. T., & da Costa, J. C. (2019). Activated peripheral blood mononuclear cell mediators trigger astrocyte reactivity. *Brain, Behavior, and Immunity*, *80*, 879–888.
- Benowitz, L. I., & Routtenberg, A. (1997). GAP-43: An intrinsic determinant of neuronal development and plasticity. *Trends in Neurosciences*, *20*, 84–91.
- Berlot, R., Metzler-Baddeley, C., Ikram, M. A., Jones, D. K., & O'Sullivan, M. J. (2016). Global efficiency of structural networks mediates cognitive control in mild cognitive impairment. *Frontiers in Aging Neuroscience*, *8*, 1–11.
- Bhadbhade, A., & Cheng, D. W. (2012). Amyloid precursor protein processing in Alzheimer's disease. *Iranian Journal of Child Neurology*, *6*(1), 1–5.
- Bogdanovic, N., Davidsson, P., Volkman, I., Winblad, B., & Blennow, K. (2000). Growth-associated protein GAP-43 in the frontal cortex and in the hippocampus in Alzheimer's disease: An immunohistochemical and quantitative study. *Journal of Neural Transmission*, *107*, 463–478.
- Brekke, E., Berger, H. R., Widerøe, M., Sonnewald, U., & Morken, T. S. (2017). Glucose and intermediary metabolism and astrocyte-neuron interactions following neonatal hypoxia-ischemia in rat. *Neurochemical Research*, *42*, 115–132.
- Brekke, E. M. F., Morken, T. S., Widerøe, M., Håberg, A. K., Brubakk, A. M., & Sonnewald, U. (2014). The pentose phosphate pathway and pyruvate carboxylation after neonatal hypoxic-ischemic brain injury. *Journal of Cerebral Blood Flow and Metabolism*, *34*, 724–734. <https://doi.org/10.1038/jcbfm.2014.8>
- Cai, J., Tuong, C. M., Zhang, Y., Shields, C. B., Guo, G., Fu, H., & Gozal, D. (2012). Mouse intermittent hypoxia mimicking apnoea of prematurity: Effects on myelinogenesis and axonal maturation. *The Journal of Pathology*, *226*, 495–508. <https://doi.org/10.1002/path.2980>
- Camandola, S., & Mattson, M. P. (2017). Brain metabolism in health, aging, and neurodegeneration. *EMBO Journal*, *36*, 1474–1492. <https://doi.org/10.15252/embj.201695810>
- Chen, Y., Zhao, C., Zhang, C., Luo, L., & Yu, G. (2012). Influence of chronic intermittent hypoxia on growth associated protein 43 expression in the hippocampus of young rats. *Neural Regen. Res.*, *7*, 1241–1246.
- Chiaravalloti, A., Micarelli, A., Ricci, M., Pagani, M., Ciccariello, G., Bruno, E., Alessandrini, M., & Schillaci, O. (2019). Evaluation of task-related brain activity: Is there a role for 18F FDG-PET imaging?. *BioMed Research International*, *1*–10. <http://dx.doi.org/10.1155/2019/4762404>
- Chugani, H. T., Phelps, M. E., & Mazziotta, J. C. (1987). Positron emission tomography study of human brain functional development. *Annals of Neurology*, *22*, 487–497.
- Coleman, P. D., Kazee, A. M., Lapham, L., Eskin, T., & Rogers, K. (1992). Reduced GAP-43 message levels are associated with increased neurofibrillary tangle density in the frontal association cortex (area 9) in Alzheimer's disease. *Neurobiology of Aging*, *13*, 631–639.
- Costantini, L. C., Barr, L. J., Vogel, J. L., & Henderson, S. T. (2008). Hypometabolism as a therapeutic target in Alzheimer's disease. *BMC Neuroscience*, *9*, 1–9. <https://doi.org/10.1186/1471-2202-9-S2-S16>
- Couto-Pereira, N. D. S., Lampert, C., Vieira, A. D. S., Lazzaretti, C., Kincheski, G. C., Espejo, P. J., Molina, V. A., Quillfeldt, J. A., & Dalmaz, C. (2019). Resilience and vulnerability to trauma: Early life interventions modulate aversive memory reconsolidation in the dorsal hippocampus. *Frontiers in Molecular Neuroscience*, *12*, 134.
- Cunnane, S., Nugent, S., Roy, M., Courchesne-Loyer, A., Croteau, E., Tremblay, S., Castellano, A., Pifferi, F., Bocti, C., Paquet, N., & Begdouri, H. (2011). Brain fuel metabolism, aging, and Alzheimer's disease. *Nutrition*, *27*, 3–20.
- Dennis, M., Spiegler, B. J., Juraneck, J. J., Bigler, E. D., Snead, O. C., & Fletcher, J. M. (2013). Age, plasticity, and homeostasis in childhood brain disorders. *Neuroscience and Biobehavioral Reviews*, *37*, 2760–2773.
- Durán-Carabali, L., Arcego, D., Odorcyk, F., Reichert, L., Cordeiro, J., Sanches, E., Freitas, L., Dalmaz, C., Pagnussat, A., & Netto, C. (2017). Prenatal and early postnatal environmental enrichment reduce acute cell death and prevent neurodevelopment and memory impairments in rats submitted to neonatal hypoxia ischemia. *Molecular Neurobiology*, *55*, 3627–3641.
- Durán-Carabali, L., Arcego, D., Sanches, E., Odorcyk, F., Marques, M., Tosta, A., Reichert, L., Carvalho, A. S., Dalmaz, C., & Netto, C. (2019). Preventive and therapeutic effects of environmental enrichment in Wistar rats submitted to neonatal hypoxia-ischemia. *Behavioral Brain Research*, *359*, 485–497.
- Faa, G., Marcalis, M., Ravarino, A., Piras, M., Pintus, M., & Fanos, V. (2014). Fetal programming of the human brain: Is there a link with insurgence of neurodegenerative disorders in adulthood? *Current Medicinal Chemistry*, *21*, 3854–3876.
- Fan, L. W., Lin, S., Pang, Y., Lei, M., Zhang, F., Rhodes, P. G., & Cai, Z. (2005). Hypoxia-ischemia induced neurological dysfunction and brain injury in the neonatal rat. *Behavioral Brain Research*, *165*, 80–90.
- Fan, X., van Bel, F., van der Kooij, M. A., Heijnen, C. J., & Groenendaal, F. (2013). Hypothermia and erythropoietin for neuroprotection after neonatal brain damage. *Pediatric Research*, *73*, 18–23.
- Golub, Y., Kaltwasser, S. F., Mauch, C. P., Herrmann, L., Schmidt, U., Holsboer, F., Czisch, M., & Wotjak, C. T. (2011). Reduced hippocampus volume in the mouse model of posttraumatic stress disorder. *Journal of Psychiatric Research*, *45*, 650–659.
- Grefkes, C., & Ward, N. S. (2014). Cortical reorganization after stroke: How much and how functional? *Neuroscientist*, *20*, 56–70.
- Hartl, D., Rohe, M., Mao, L., Staufienbiel, M., Zabel, C., & Klose, J. (2008). Impairment of adolescent hippocampal plasticity in a mouse model for Alzheimer's disease precedes disease phenotype. *PLoS One*, *3*, e2759.
- Hassell, K. J., Ezzati, M., Alonso-Alconada, D., Hausenloy, D. J., & Robertson, N. J. (2015). New horizons for newborn brain protection: Enhancing endogenous neuroprotection. *Archives of Disease in Childhood-Fetal and Neonatal Edition*, *100*, F541–F552.
- He, C., Tshipis, C. P., LaManna, J. C., & Xu, K. (2017). Environmental enrichment induces increased cerebral capillary density and improved cognitive function in mice. In H. Halpern, J. LaManna, & D. E. B. Harrison (Eds.), *Oxygen Transport to Tissue XXXIX. Advances in Experimental Medicine and Biology*, Vol. 977, (pp. 175–181). Springer, Cham.
- Hefter D., & Draguhn A. (2017). APP as a Protective Factor in Acute Neuronal Insults. *Frontiers in Molecular Neuroscience*, *10*, <http://dx.doi.org/10.3389/fnmol.2017.00022>.
- Hefter, D., Kaiser, M., Weyer, S. W., Papageorgiou, I. E., Both, M., Kann, O., Müller, U. C., & Draguhn, A. (2016). Amyloid precursor protein protects neuronal network function after hypoxia via control of voltage-gated calcium channels. *Journal of Neuroscience*, *36*, 8356–8371.

- Hefter, D., Ludewig, S., Korte, M., & Draguhn, A. (2019). Amyloid, APP, and electrical activity of the brain. *The Neuroscientist*, 26, 231–251.
- Herring, A., Lewejohann, L., Panzer, A. L., Donath, A., Kröll, O., Sachser, N., Paulus, W., & Keyvani, K. (2011). Preventive and therapeutic types of environmental enrichment counteract beta amyloid pathology by different molecular mechanisms. *Neurobiology of Diseases*, 42, 530–538.
- Higaki, A., Mogi, M., Iwanami, J., Min, L. J., Bai, H. Y., Shan, B. S., Kan-no, H., Ikeda, S., Higaki, J., & Horiuchi, M. (2018). Recognition of early stage thigmotaxis in morris water maze test with convolutional neural network. *PLoS One*, 13.
- Hill, C. A., & Fitch, R. H. (2012). Sex differences in mechanisms and outcome of neonatal hypoxia-ischemia in rodent models: Implications for sex-specific neuroprotection in clinical neonatal practice. *Neurology Research International*, 2012, 12–14.
- Holahan, M. R., Honegger, K. S., Tabatadze, N., & Routtenberg, A. (2007). GAP-43 gene expression regulates information storage. *Learning & Memory*, 14, 407–415.
- Horwitz, B., Grady, C. L., Schlageter, N. L., Duara, R., & Rapoport, S. I. (1987). Intercorrelations of regional cerebral glucose metabolic rates in Alzheimer's disease. *Brain Research*, 407, 294–306.
- Huang, S. Y., Hsu, J. L., Lin, K. J., Liu, H. L., Wey, S. P., Hsiao, I. T., Weiner, M. et al (2018). Characteristic patterns of inter- and intra-hemispheric metabolic connectivity in patients with stable and progressive mild cognitive impairment and Alzheimer's disease. *Scientific Reports*, 8, 1–11.
- Huang, Z., Liu, J., Cheung, P. Y., & Chen, C. (2009). Long-term cognitive impairment and myelination deficiency in a rat model of perinatal hypoxic-ischemic brain injury. *Brain Research*, 1301, 100–109. <https://doi.org/10.1016/j.brainres.2009.09.006>
- Illouz, T., Madar, R., Louzon, Y., Griffioen, K. J., & Okun, E. (2016). Unraveling cognitive traits using the Morris water maze unbiased strategy classification (MUST-C) algorithm. *Brain, Behavior, and Immunity*, 52, 132–144.
- Jack, C. R., Bennett, D. A., Blennow, K., Carrillo, M. C., Dunn, B., Haeberlein, S. B., Holtzman, D. M., Jagust, W., Jessen, F., Karlawish, J., Liu, E., Molinuevo, J. L., Montine, T., Phelps, C., Rankin, K. P., Rowe, C. C., Scheltens, P., Siemers, E., Snyder, H. M., ... Silverberg, N. (2018). NIA-AA Research Framework: Toward a biological definition of Alzheimer's disease. *Alzheimer's & Dementia*, 14, 535–562. <https://doi.org/10.1016/j.jalz.2018.02.018>
- Kang, H., Choi, D. H., Kim, S. K., Lee, J., & Kim, Y. J. (2016). Alteration of energy metabolism and antioxidative processing in the hippocampus of rats reared in long-term environmental enrichment. *Developmental Neuroscience*, 38, 186–194.
- Kempermann, G. (2019). Environmental enrichment, new neurons and the neurobiology of individuality. *Nature Reviews Neuroscience*, 20(4), 235–245.
- Koo, J. W., Park, C. H., Choi, S. H., Kim, N. J., Kim, H., Choe, C., Suh, Y., Creative, N., & National, S. (2003). Postnatal environment can counteract prenatal effects on cognitive ability, cell proliferation, and synaptic protein expression. *The FASEB Journal*. <https://doi.org/10.1096/fj.02-1032fje>
- Marik, J., Ogasawara, A., Martin-McNulty, B., Ross, J., Flores, J. E., Gill, H. S., Tinianow, J. N. et al (2009). PET of glial metabolism using 2-18F-FLUOROACETATE. *Journal of Nuclear Medicine*, 50, 982–990.
- Martin, A., Rojas, S., Pareto, D., Santalucia, T., Millan, O., Abasolo, I., Gomez, V., Llop, J., Gispert, J. D., Falcon, C., & Bargalló, N. (2009). Depressed glucose consumption at reperfusion following brain ischemia does not correlate with mitochondrial dysfunction and development of infarction: An in vivo positron emission tomography study. *Current Neurovascular Research*, 6, 82–88.
- Martin, L. J., Wong, M., & Hanaford, A. (2019). Neonatal brain injury and genetic causes of adult-onset neurodegenerative disease in mice interact with effects on acute and late outcomes. *Frontiers in Neurology*, 10, 635.
- Masliah, E., Mallory, M., Hansen, L., Alford, M., DeTeresa, R., Terry, R., Baudier, J., & Saitoh, T. (1992). Localization of amyloid precursor protein in GAP43-immunoreactive aberrant sprouting neurites in Alzheimer's disease. *Brain Research*, 574, 312–316. [https://doi.org/10.1016/0006-8993\(92\)90831-5](https://doi.org/10.1016/0006-8993(92)90831-5)
- Masliah, E., & Terry, R. (1993). The role of synaptic proteins in the pathogenesis of disorders of the central nervous system. *Brain Pathology*, 3, 77–85. <https://doi.org/10.1111/j.1750-3639.1993.tb00728.x>
- McDonald, M. W., Hayward, K. S., Rosbergen, I. C. M., Jeffers, M. S., & Corbett, D. (2018). Is environmental enrichment ready for clinical application in human post-stroke rehabilitation? *Frontiers in Behavioural Neurosciences*, 12, 1–16.
- McKenna, M. C., Scafidi, S., & Robertson, C. L. (2015). Metabolic alterations in developing brain after injury: Knowns and unknowns. *Neurochemical Research*, 40, 2527–2543. <https://doi.org/10.1007/s11064-015-1600-7>
- McQuillen, P. S., Vannucci, S. J., & Hagberg, H. (2017). Pathophysiology of hypoxic-ischemic brain injury. In R. A. Polin, S. H. Abman, D. H. Rowitch, W. E. Benitz, & W. W. Fox (Eds.), *Fetal and Neonatal Physiology (Fifth Edition)*. Elsevier Inc.
- Millar, L. J., Shi, L., Hoerder-Suabedissen, A., & Molnár, Z. (2017) Neonatal hypoxia ischaemia: Mechanisms, models, and therapeutic challenges. *Frontiers in Cellular Neuroscience*, 11, 78.
- Nalivaeva, N. N., Fisk, L., Aviles, R. M. C., Plesneva, S. A., Zhuravin, I. A., & Turner, A. J. (2003). Effects of prenatal hypoxia on expression of amyloid precursor protein and metalloproteinases in the rat brain. *Letters in Peptide Science*, 10, 455–462.
- Nalivaeva, N. N., Turner, A. J., & Zhuravin, I. A. (2018). Role of prenatal hypoxia in brain development, cognitive functions, and neurodegeneration. *Frontiers in Neuroscience*, 12, 1–21.
- Nehlig, A. (2004). Brain uptake and metabolism of ketone bodies in animal models. *Prostaglandins, Leukotrienes and Essential Fatty Acids*, 70(3), 265–275.
- Netto, C. A., Hodges, H., Sinden, J. D., Le Peillet, E., Kershaw, T., Sowinski, P., Meldrum, B. S., & Gray, J. A. (1993). Effects of fetal hippocampal field grafts on ischaemic-induced deficits in spatial navigation in the water maze. *Neuroscience*, 54, 69–92. [https://doi.org/10.1016/0306-4522\(93\)90384-R](https://doi.org/10.1016/0306-4522(93)90384-R)
- Netto, C., Sanches, E., Odorczyk, F., Duran-Carabali, L., & Sizonenko, S. (2018). Pregnancy as a valuable period for preventing hypoxia-ischemia brain damage. *International Journal of Developmental Neuroscience*, 70(1), 12–24.
- Netto, C. A., Sanches, E., Odorczyk, F. K., Duran-Carabali, L. E., & Weis, S. N. (2017). Sex-dependent consequences of neonatal brain hypoxia-ischemia in the rat. *Journal of Neuroscience Research*, 95, 409–421.
- Odahara, T. (2004). Stability and solubility of integral membrane proteins from photosynthetic bacteria solubilized in different detergents. *Biochimica Et Biophysica Acta (BBA) - Biomembranes*, 1660, 80–92. <https://doi.org/10.1016/j.bbamem.2003.11.003>
- Odorczyk, F. K., Duran-carabali, L. E., Rocha, D. S., Sanches, E. F., Martini, A. P., & Venturin, G. T. (2020). Differential glucose and beta-hydroxybutyrate metabolism confers an intrinsic neuroprotection to the immature brain in a rat model of neonatal hypoxia ischemia. *Experimental Neurology*, 330, 113317.
- Rafiki, A., Boulland, J. L., Halestrap, A. P., Ottersen, O. P., & Bergersen, L. (2003). Highly differential expression of the monocarboxylate transporters MCT2 and MCT4 in the developing rat brain. *Neuroscience*, 122, 677–688. <https://doi.org/10.1016/j.neuroscience.2003.08.040>
- Rojas, J. J., Deniz, B. F., Miguel, P. M., Diaz, R., Hermel, É. D. E. S., Achaval, M., Netto, C. A., & Pereira, L. O. (2013). Effects of daily environmental enrichment on behavior and dendritic spine density in hippocampus following neonatal hypoxia-ischemia in the rat.



- Experimental Neurology*, 241, 25–33. <https://doi.org/10.1016/j.expneurol.2012.11.026>
- Rubinov, M., & Sporns, O. (2010). Complex network measures of brain connectivity: Uses and interpretations. *NeuroImage*, 52, 1059–1069. <https://doi.org/10.1016/j.neuroimage.2009.10.003>
- Rumajogee, P., Bregman, T., Miller, S. P., Yager, J. Y., & Fehlings, M. G. (2016). Rodent hypoxia–ischemia models for cerebral palsy research: A systematic review. *Frontiers in Neurology*, 7, 57.
- Sale, A. (2018). A systematic look at environmental modulation and its impact in brain development. *Trends in Neurosciences*, 41, 4–17. <https://doi.org/10.1016/j.tins.2017.10.004>
- Salminen, A., Kauppinen, A., & Kaarniranta, K. (2017). Hypoxia/ischemia activate processing of amyloid precursor protein: Impact of vascular dysfunction in the pathogenesis of Alzheimer's disease. *Journal of Neurochemistry*, 140, 536–549. <https://doi.org/10.1111/jnc.13932>
- Sanchez, E. F., Arteni, N. S., Nicola, F., Boisserand, L., Willborn, S., & Netto, C. (2013). Early hypoxia-ischemia causes hemisphere and sex-dependent cognitive impairment and histological damage. *Neuroscience*, 237, 208–215. <https://doi.org/10.1016/j.neurosci.2013.01.066>
- Seddon, A. M., Curnow, P., & Booth, P. J. (2004). Membrane proteins, lipids and detergents: not just a soap opera. *Biochimica Et Biophysica Acta (BBA) - Biomembranes*, 1666(1–2), 105–117.
- Selvi, Y., Gergerlioglu, H. S., Akbaba, N., Oz, M., Kandeger, A., Demir, E. A., Yerlikaya, F. H., & Nurullahoglu-Atalik, K. E. (2017). Impact of enriched environment on production of tau, amyloid precursor protein and amyloid- β peptide in high-fat and high-sucrose-fed rats. *Acta Neuropsychiatr.*, 29, 291–298. <https://doi.org/10.1017/neu.2016.63>
- Shi, Y., Zhao, J. N., Liu, L., Hu, Z. X., Tang, S. F., Chen, L., & Jin, R. B. (2012). Changes of positron emission tomography in newborn infants at different gestational ages, and neonatal hypoxic-ischemic encephalopathy. *Pediatric Neurology*, 46, 116–123.
- Sokoloff, L. (1993). Sites and mechanisms of function-related changes in energy metabolism in the nervous system. *Developmental Neuroscience*, 15, 194–206.
- Sparling, J. E., Mahoney, M., Baker, S., & Bielajew, C. (2010). The effects of gestational and postpartum environmental enrichment on the mother rat: A preliminary investigation. *Behavioral Brain Research*, 208, 213–223. <https://doi.org/10.1016/j.bbr.2009.11.041>
- Stadlin, A., James, A., Fiscus, R., Wong, Y. F., Rogers, M., & Haines, C. (2003). Development of a postnatal 3-day-old rat model of mild hypoxic-ischemic brain injury. *Brain Research*, 993, 101–110. <https://doi.org/10.1016/j.brainres.2003.08.058>
- Stoessl, A. (2017). Glucose utilization: Still in the synapse. *Nature Neuroscience*, 20, 382–384.
- Stokin, G. B., & Goldstein, L. S. B. (2006). Axonal transport and Alzheimer's disease. *Annual Review of Biochemistry*, 75, 607–627. <https://doi.org/10.1146/annurev.biochem.75.103004.142637>
- Sun, J. Q., Cao, Y. T., Liu, H. Q., & Deng, W. A. (2007). Neuroprotective effects of exogenous basic fibroblast growth factor on the hypoxic-ischemic brain damage of neonatal rats. *Zhonghua Er Ke Za Zhi.*, 45, 354–359.
- Tang, M., Gao, G., Rueda, C. B., Yu, H., Thibodeaux, D. N., Awano, T., Engelstad, K. M., Sanchez-Quintero, M.-J., Yang, H., Li, F., Li, H., Su, Q., Shetler, K. E., Jones, L., Seo, R., McConathy, J., Hillman, E. M., Noebels, J. L., De Vivo, D. C., & Monani, U. R. (2017). Brain microvasculature defects and Glut1 deficiency syndrome averted by early repletion of the glucose transporter-1 protein. *Nature Communications*, 8(1), 1–15.
- Thorngren-Jerneck, K., Ley, D., Hellström-Westas, L., Hernandez-Andrade, E., Lingman, G., Ohlsson, T., Oskarsson, G., Pesonen, E., Sandell, A., Strand, S.-E., Werner, O., & Maršal, K. (2001). Reduced postnatal cerebral glucose metabolism measured by PET after asphyxia in near term fetal lambs. *Journal of Neuroscience Research*, 66, 844–850. <https://doi.org/10.1002/jnr.10051>
- Torigian, D. A., Kjaer, A., Zaidi, H., & Alavi, A. (2016). PET/MRI: Clinical applications. *PET Clinics*, 11(4), xi–xii.
- Treit D. & Fundytus M. (1988). Thigmotaxis as a test for anxiolytic activity in rats. *Pharmacology, Biochemistry and Behavior*, 31, 959–962.
- Vannucci, S. J., Reinhart, R., Maher, F., Bondy, C. A., Lee, W.-H., Vannucci, R. C., & Simpson, I. A. (1998). Alterations in GLUT1 and GLUT3 glucose transporter gene expression following unilateral hypoxia-ischemia in the immature rat brain. *Brain Research. Developmental Brain Research*, 107, 255–264. [https://doi.org/10.1016/S0165-3806\(98\)00021-2](https://doi.org/10.1016/S0165-3806(98)00021-2)
- Verklan, T. (2009). The chilling details: Hypoxic-ischemic encephalopathy. *The Journal of Perinatal & Neonatal Nursing*, 23, 59–68.
- Vorhees, C. V., & Williams, M. T. (2006). Morris water maze: Procedures for assessing spatial and related forms of learning and memory. *Nature Protocols*, 1, 848–858. <https://doi.org/10.1038/nprot.2006.116>
- Waddell, J., Hanscoma, M., Edwards, N. S., McKenna, M. C., & McCarthy, M. M. (2016). Sex differences in cell genesis, hippocampal volume and behavioral outcomes in a rat model of neonatal HI. *Experimental Neurology*, 275, 285–295.
- Wang, C. J., Wu, Y., Zhang, Q., Yu, K. W., & Wang, Y. Y. (2019). An enriched environment promotes synaptic plasticity and cognitive recovery after permanent middle cerebral artery occlusion in mice. *Neural Regeneration Research*, 14, 462–469.
- Winkler, E. A., Nishida, Y., Sagare, A. P., Rege, S. V., Bell, R. D., Perlmutter, D., Sengillo, J. D., Hillman, S., Kong, P., Nelson, A. R., & Sullivan, J. S. (2015). GLUT1 reductions exacerbate Alzheimer's disease vasculo-neuronal dysfunction and degeneration. *Nature Neuroscience*, 18, 521–530.
- Wu, Y., Zhang, S., Xu, Q., Zou, H., Zhou, W., Cai, F., Li, T., & Song, W. (2016). Regulation of global gene expression and cell proliferation by APP. *Scientific Reports*, 6(1), 1–9.
- Yang, S. N., & Lai, M. C. (2011). Perinatal hypoxic-ischemic encephalopathy. *Journal of Biomedicine and Biotechnology*, 2011, 1–6.
- Zanirati, G., Azevedo, P. N., Venturin, G. T., Greggio, S., Alcará, A. M., Zimmer, E. R., Feltes, P. K., & DaCosta, J. C. (2018). Depression comorbidity in epileptic rats is related to brain glucose hypometabolism and hypersynchronicity in the metabolic network architecture. *Epilepsia*, 59, 923–934. <https://doi.org/10.1111/epi.14057>
- Zhang, M., Wu, J., Huo, L., Luo, L., Song, X., Fan, F., Lu, Y., & Liang, D. (2016). Environmental enrichment prevent the juvenile hypoxia-induced developmental loss of parvalbumin-immunoreactive cells in the prefrontal cortex and neurobehavioral alterations through inhibition of NADPH oxidase-2-derived oxidative stress. *Molecular Neurobiology*, 53, 7341–7350. <https://doi.org/10.1007/s12035-015-9656-6>
- Zhang, Z., Zhang, H., Du, B., & Chen, Z. (2012). Enriched environment upregulates growth-associated protein 43 expression in the hippocampus and enhances cognitive abilities in prenatally stressed rat offspring. *Neural Regeneration Research*, 7, 1967–1973.
- Zhao, W., Belayev, L., & Ginsberg, M. D. (1997). Transient middle cerebral artery occlusion by intraluminal suture: II. Neurological deficits, and pixel-based correlation of histopathology with local blood flow and glucose utilization. *Journal of Cerebral Blood Flow and Metabolism*, 17, 1281–1290. <https://doi.org/10.1097/00004647-199712000-00003>
- Zhou, J., Zhou, T., Cao, R., Liu, Z., Shen, J., Chen, P., Wang, X., & Liang, S. (2006). Evaluation of the application of sodium deoxycholate to proteomic analysis of rat hippocampal plasma membrane. *Journal of Proteome Research*, 5, 2547–2553. <https://doi.org/10.1021/pr060112a>
- Zhu, X., Wang, P., Liu, H., Zhan, J., Wang, J., Li, M., Zeng, L., & Xu, P. (2019). Changes and significance of SYP and GAP-43 expression in the hippocampus of CIH rats. *International Journal of Medical Sciences*, 16, 394–402.

Zimmer, E. R., Parent, M. J., Souza, D. G., Leuzy, A., Lecrux, C., Kim, H. I., Gauthier, S., Pellerin, L., Hamel, E., & Rosa-Neto, P. (2017). [18F] FDG PET signal is driven by astroglial glutamate transport. *Nature Neuroscience*, 20, 393–395.

SUPPORTING INFORMATION

Additional supporting information may be found online in the Supporting Information section.

How to cite this article: Durán-Carabali LE, Kawa Odorczyk F, Greggio S, et al. Pre- and early postnatal enriched environmental experiences prevent neonatal hypoxia-ischemia late neurodegeneration via metabolic and neuroplastic mechanisms. *J Neurochem*. 2021;157:1911–1929. <https://doi.org/10.1111/jnc.15221>